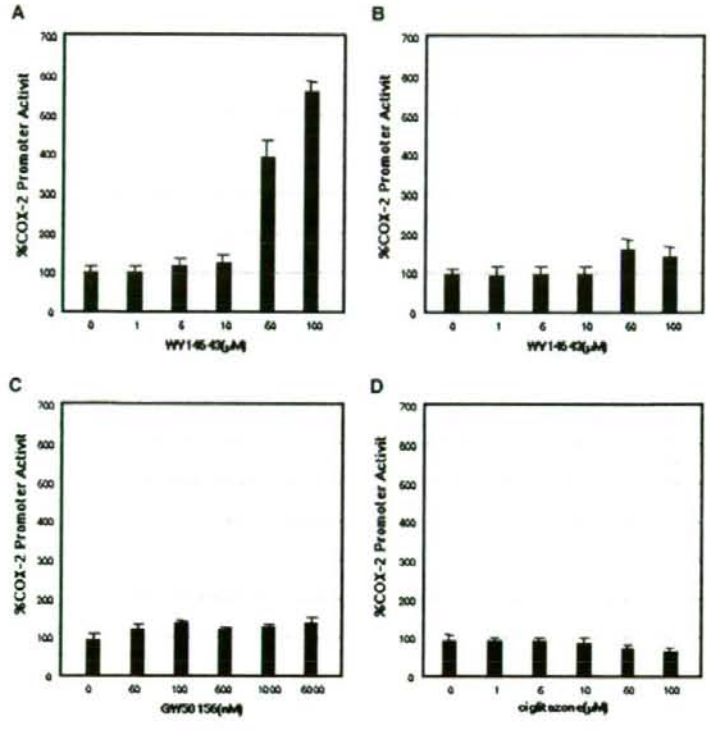

Fig. 6A–D. PPARα-specific agonist increases in the transcriptional activity of the *COX-2* gene. **A, B** HCT116 cells were cotransfected with 3 μg of human *COX-2* promoter construct (−1555/+178) (**A**) or mutant construct of the CRE site in the *COX-2* promoter (**B**) and 20 ng pRL-TK. Following transfection, cells were treated with various concentrations of WY14643 (0, 1, 5, 10, 50, or 100 μM) for 24 h and then the luciferase activities were measured. *Columns*, means; *bars*, SD; $n = 4$. **C, D** HCT116 cells were cotransfected with 3 μg of human *COX-2* promoter construct (−1555/+178) and 20 ng pRL-TK. Following transfection, cells were treated with various concentrations of GW501516 (0, 50, 100, 500, 1000, or 5000 nM) (**C**) or ciglitazone (0, 1, 5, 10, 50, or 100 μM) (**D**) for 24 h and then the luciferase activities were measured. *Columns*, means; *bars*, SD; $n = 4$

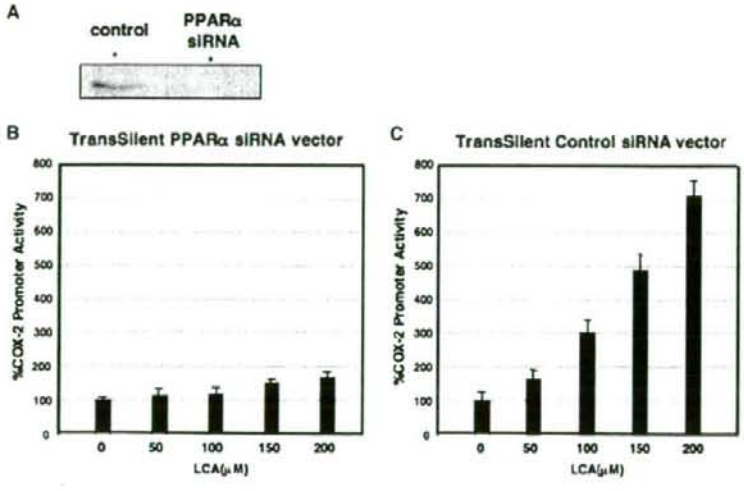

Fig. 7A–C. PPARα siRNA inhibits LCA-mediated induction of *COX-2*. **A** Western blot analysis of endogenous PPARα protein levels, transfected with Control siRNA vectors into HCT116 cells (*lane 1*) and transfected with TransSilent PPARα siRNA vectors (*lane 2*). **B, C** HCT116 cells were cotransfected with 3 μg of human *COX-2* promoter construct (−1555/+178), 20 ng of pRL-TK, and 5 μg of PPARα SiRNA vector (**B**) or control siRNA vector (**C**). There were no effects by the addition of LCA to activate the *COX-2* promoter. *Columns*, means; *bars*, SD; $n = 4$

First, we examined the effects of bile acids on the transcriptional activity of the *COX-2* gene. Transient transfection experiments clearly showed that LCA, DCA, and CDCA (200 μM) increased the transcriptional activity of the *COX-2* gene in HCT116 cells. In contrast, neither TCA, CA, nor conjugated bile acids caused any change in the rate of *COX-2* transcription. We obtained the same results in another colon cancer cell line, HT29, indicating that LCA, DCA, and CDCA might be generally involved in the activation of the

COX-2 gene. LCA is a secondary bile acid generated by bacteria in the colon. The fecal level of LCA is higher than that of other secondary bile acids in patients with colorectal cancer,[45] and a high-fat diet is associated with an increase in the excretion of fecal bile acids.[46] The secondary bile acid LCA has been thought to be the most toxic,[29] and LCA can also promote colon cancer in experimental animals.[24]

To reveal the involvement of LST-2 in *COX-2* induction, transfection experiments were carried out in LST-2-deficient HepG2 cells and an adenovirus expression system. *COX-2* promoter activities were upregulated by bile acids in LST-2-expressing GepG2 cells, whereas bile acids did not upregulate *COX-2* promoter in LST-2-deficient cells. The present data showed that LST-2 plays an important role in bile acid-induced *COX-2* expression. These data indicate that LST-2 acts as an uptake transporter to deliver bile acids into the cell and takes part in bile acid-induced *COX-2* expression in human colonic cancer cells. Direct evidence for the uptake of bile acids by cancer cells may be obtained by uptake experiments. Until now, the reason for the strong expression of LST-2 in gastrointestinal cancers has been unknown. As we reported previously, *LST-2* gene expression is also positively regulated by bile acids.[47] Our data suggest LST-2 transports LCA into cancer cells and induces the expression of *COX-2*. Most secondary bile acids are generated in the colon. In the normal colorectal mucosa, expression of LST-2 is very rare. From our present data, we speculate that under normal circumstances, without the expression of LST-2, very few secondary bile acids are taken up into the colorectal mucosal cells. By contrast, in colorectal cancer cells, secondary bile acids, LCA or DCA, are easily taken up by the cells and induce the expression of *COX-2*. LST-2 thus plays important roles in the proliferation or carcinogenesis of the colorectal cancer cells by regulating the expression of *COX-2*.

In order to elucidate the main transactivation domain induced by LCA in the *COX-2* promoter, we performed transfection analyses in HCT116 cells using different deletion mutants and then exposed the cells to LCA. Our results indicate that the LCA-dependent induction of the *COX-2* gene is complex and may involve some transcription factors binding to C/EBP and CRE elements (Figs. 3, 4).

Because the CRE and C/EBP sites of the *COX-2* promoter were important for the inductive effects of LCA, we preformed EMSAs to identify the transcriptional factors. The EMSA results showed a positive correlation between the concentration of LCA and the amount of DNA binding protein binding to the CRE site of *COX-2* (Fig. 5A). In contrast, the C/EBP binding sites showed no significant change in response to LCA (Fig. 5B). This result indicated that the CRE binding site might be essential in the LCA-dependent induction of the *COX-2* gene. Interestingly, supershift assays revealed CREB and PPARα to be involved in the DNA binding complex (Fig. 5C). These findings are consistent with those of previous reports in which CREB was found to be important for the induction of *COX-2* in human cancer and normal cells.[48,49] However, little is known about the ability of PPARα to mediate the transcriptional activation of *COX-2*. Treatment of HCT116 cells with the PPARα agonist WY14643 resulted in a 5.6-fold induction increase, while mutagenizing the CRE site caused a decrease in the loss of responsiveness to LCA (Fig. 6A, B). In contrast, neither the PPARβ/δ agonist GW501516 nor the PPARγ agonist ciglitazone caused any change in the rate of *COX-2* transcription (Fig. 6C, D). Furthermore, specific downregulation of *PPARα* mRNA by Trans-Silent PPARα siRNA vectors suppressed this induction (Fig. 7B). These results strongly suggest that the CRE binding site is essential in the *COX-2* gene activation induced by PPARα, and that PPARα is a key molecule for the LCA-induced transactivation of *COX-2*. In addition, there is growing evidence that the coactivator CREB binding protein/p300 (CBP/p300) plays very important roles in the activation of gene expression by CREB.[50-52] Recent studies also suggest that transcriptional activation by CREB requires CBP/p300-interacting transactivator with ED/rich tail-2 (CITED2) as a PPARα coregulator, with the result that CREB and PPARα can bind to CITED2.[48,53] Moreover, FXR is a nuclear bile acid receptor that binds CDCA, DCA, and LCA and regulates gene transcription.[26] Furthermore, bile acids stimulate PPARα expression via the FXR response element located within the human *PPARα* promoter.[36] Moreover, it is possible that FXR is involved in the DNA binding protein that binds to the CRE site of the *COX-2* promoter, but not PXR or VDR (unpublished results). These findings provide molecular evidence for crosstalk between FXR and PPARα pathways in humans.[26,36,49,53] To our knowledge, these findings represent the first evidence that PPARα and CREB regulate LCA-mediated *COX-2* gene expression.

While our experiments were in progress, an article was published demonstrating that epidermal growth factor receptor (EGFR) is activated by bile acids and functions to induce *COX-2* expression by p42/44 and p38 mitogen-activated protein kinase (MAPK) cascades.[54] This EGFR/MAPK cascade increases the expression of *c-fos* and *c-jun* and the binding activity of AP-1 (a transcription factor consisting of *c-fos* and *c-jun* protein complexes) to the CRE site, and finally the AP-1 complexes transactivate the *COX-2* promoter, increasing expression of *COX-2* mRNA.[54,55] According to our data, we propose that bile acids activate *COX-2* expres-

sion via another signaling pathway involving PPARα/CREB binding to the CRE site. In addition, our data also indicate that LST-2 transports bile acids into HCT116 cells, consequently causing activation of the *COX-2* promoter by the formation of a protein–DNA complex including PPARα and CREB.

In summary, our data strongly suggest that LCA transported by LST-2 into cells may be a natural ligand for transcription factors represented by PPARα and CREB, thereby activating LCA-mediated *COX-2* gene expression, and participating in the induction of *COX-2* in human colon cancer. The results provide new information regarding the growth-modifying potential of LCA in colon cancer, and the role of the bile acid transporter LST-2/OATP8/OATP1B3, which is strongly expressed in gastrointestinal cancers.

Acknowledgment. We thank Brent Bell for reading the manuscript and Emiko Shibuya for technical assistance. This work was supported in part by research grants from the Ministry of Education, Culture, Sports, Science and Technology of Japan, the Takeda Foundation, and the Sankyo Foundation.

References

1. Abe T, Unno M, Onogawa T, Tokui T, Kondo TN, Nakagomi R, et al. LST-2, a human liver-specific organic anion transporter, determines methotrexate sensitivity in gastrointestinal cancers. Gastroenterology 2001;120:1689–99.
2. Abe T, Kakyo M, Tokui T, Nakagomi R, Nishio T, Nakai D, et al. Identification of a novel gene family encoding human liver-specific organic anion transporter LST-1. J Biol Chem 1999;274: 17159–63.
3. Rosenberg L, Palmer JR, Zauber AG, Warshauer ME, Stolley PD, Shapiro S. A hypothesis: nonsteroidal anti-inflammatory drugs reduce the incidence of large-bowel cancer. J Natl Cancer Inst 1991;83:355–8.
4. Reddy BS, Rao CV, Seibert K. Evaluation of cyclooxygenase-2 inhibitor for potential chemopreventive properties in colon carcinogenesis. Cancer Res 1996;56:4566–9.
5. Fu SL, Wu YL, Zhang YP, Qiao MM, Chen Y. Anti-cancer effects of COX-2 inhibitors and their correlation with angiogenesis and invasion in gastric cancer. World J Gastroenterol 2004;10:1971–4.
6. Thun MJ, Namboodiri MM, Heath CW Jr. Aspirin use and reduced risk of fatal colon cancer. N Engl J Med 1991;325: 1593–6.
7. Logan RF, Little J, Hawtin PG, Hardcastle JD. Effect of aspirin and non-steroidal anti-inflammatory drugs on colorectal adenomas: case–control study of subjects participating in the Nottingham faecal occult blood screening programme. BMJ 1993;307: 285–9.
8. Schreinemachers DM, Everson RB. Aspirin use and lung, colon, and breast cancer incidence in a prospective study. Epidemiology 1994;5:138–46.
9. Smith WL, Garavito RM, DeWitt DL. Prostaglandin endoperoxide H synthases (cyclooxygenases)-1 and -2. J Biol Chem 1996;271:33157–60.
10. Kujubu DA, Fletcher BS, Varnum BC, Lim RW, Herschman HR. TIS10, a phorbol ester tumor promoter-inducible mRNA from Swiss 3T3 cells, encodes a novel prostaglandin synthase/cyclooxygenase homologue. J Biol Chem 1991;266:12866–72.
11. Jones DA, Carlton DP, McIntyre TM, Zimmerman GA, Prescott SM. Molecular cloning of human prostaglandin endoperoxide synthase type II and demonstration of expression in response to cytokines. J Biol Chem 1993;268:9049–54.
12. DuBois RN, Awad J, Morrow J, Roberts LJ 2nd, Bishop PR. Regulation of eicosanoid production and mitogenesis in rat intestinal epithelial cells by transforming growth factor-alpha and phorbol ester. J Clin Invest 1994;93:493–8.
13. Inoue H, Yokoyama C, Hara S, Tone Y, Tanabe T. Transcriptional regulation of human prostaglandin-endoperoxide synthase-2 gene by lipopolysaccharide and phorbol ester in vascular endothelial cells. Involvement of both nuclear factor for interleukin-6 expression site and cAMP response element. J Biol Chem 1995;270:24965–71.
14. Subbaramaiah K, Telang N, Ramonetti JT, Araki R, DeVito B, Weksler BB, et al. Transcription of cyclooxygenase-2 is enhanced in transformed mammary epithelial cells. Cancer Res 1996;56: 4424–9.
15. Mestre JR, Subbaramaiah K, Sacks PG, Schantz SP, Tanabe T, Inoue H, et al. Retinoids suppress epidermal growth factor-induced transcription of cyclooxygenase-2 in human oral squamous carcinoma cells. Cancer Res 1997;57:2890–5.
16. Eberhart CE, Coffey RJ, Radhika A, Giardiello FM, Ferrenbach S, DuBois RN. Up-regulation of cyclooxygenase 2 gene expression in human colorectal adenomas and adenocarcinomas. Gastroenterology 1994;107:1183–8.
17. Gupta RA, Dubois RN. Colorectal cancer prevention and treatment by inhibition of cyclooxygenase-2. Nat Rev Cancer 2001;1: 11–21.
18. Tsujii M, Kawano S, DuBois RN. Cyclooxygenase-2 expression in human colon cancer cells increases metastatic potential. Proc Natl Acad Sci USA 1997;94:3336–40.
19. Tsujii M, DuBois RN. Alterations in cellular adhesion and apoptosis in epithelial cells overexpressing prostaglandin endoperoxide synthase 2. Cell 1995;83:493–501.
20. Tsujii M, Kawano S, Tsuji S, Sawaoka H, Hori M, DuBois RN. Cyclooxygenase regulates angiogenesis induced by colon cancer cells. Cell 1998;93:705–16.
21. Masunaga R, Kohno H, Dhar DK, Ohno S, Shibakita M, Kinugasa S, et al. Cyclooxygenase-2 expression correlates with tumor neovascularization and prognosis in human colorectal carcinoma patients. Clin Cancer Res 2000;6:4064–8.
22. Chandrasekharan NV, Dai H, Roos KL, Evanson NK, Tomsik J, Elton TS, et al. COX-3, a cyclooxygenase-1 variant inhibited by acetaminophen and other analgesic/antipyretic drugs: cloning, structure, and expression. Proc Natl Acad Sci USA 2002;99: 13926–31.
23. Craven PA, Pfanstiel J, DeRubertis FR. Role of activation of protein kinase C in the stimulation of colonic epithelial proliferation and reactive oxygen formation by bile acids. J Clin Invest 1987;79:532–41.
24. Narisawa T, Magadia NE, Weisburger JH, Wynder EL. Promoting effect of bile acids on colon carcinogenesis after intrarectal instillation of *N*-methyl-*N*′-nitro-*N*-nitrosoguanidine in rats. J Natl Cancer Inst 1974;53:1093–7.
25. Allinger UG, Johansson GK, Gustafsson JA, Rafter JJ. Shift from a mixed to a lactovegetarian diet: influence on acidic lipids in fecal water—a potential risk factor for colon cancer. Am J Clin Nutr 1989;50:992–6.
26. Makishima M, Okamoto AY, Repa JJ, Tu H, Learned RM, Luk A, et al. Identification of a nuclear receptor for bile acids. Science 1999;284:1362–5.
27. Parks DJ, Blanchard SG, Bledsoe RK, Chandra G, Consler TG, Kliewer SA, et al. Bile acids: natural ligands for an orphan nuclear receptor. Science 1999;284:1365–8.
28. Staudinger JL, Goodwin B, Jones SA, Hawkins-Brown D, MacKenzie KI, LaTour A, et al. The nuclear receptor PXR is a lithocholic acid sensor that protects against liver toxicity. Proc Natl Acad Sci USA 2001;98:3369–74.

29. Makishima M, Lu TT, Xie W, Whitfield GK, Domoto H, Evans RM, et al. Vitamin D receptor as an intestinal bile acid sensor. Science 2002;296:1313–6.
30. Kersten S, Desvergne B, Wahli W. Roles of PPARs in health and disease. Nature 2000;405:421–4.
31. Meade EA, McIntyre TM, Zimmerman GA, Prescott SM. Peroxisome proliferators enhance cyclooxygenase-2 expression in epithelial cells. J Biol Chem 1999;274:8328–34.
32. Willson TM, Brown PJ, Sternbach DD, Henke BR. The PPARs: from orphan receptors to drug discovery. J Med Chem 2000;43: 527–50.
33. Desvergne B, Wahli W. Peroxisome proliferator-activated receptors: nuclear control of metabolism. Endocr Rev 1999; 20:649–88.
34. Guerre-Millo M, Gervois P, Raspe E, Madsen L, Poulain P, Derudas B, et al. Peroxisome proliferator-activated receptor alpha activators improve insulin sensitivity and reduce adiposity. J Biol Chem 2000;275:16638–42.
35. Chinetti G, Fruchart JC, Staels B. Peroxisome proliferator-activated receptors (PPARs): nuclear receptors at the crossroads between lipid metabolism and inflammation. Inflamm Res 2000;49:497–505.
36. Pineda Torra I, Claudel T, Duval C, Kosykh V, Fruchart JC, Staels B. Bile acids induce the expression of the human peroxisome proliferator-activated receptor alpha gene via activation of the farnesoid X receptor. Mol Endocrinol 2003;17:259–72.
37. Zhang F, Subbaramaiah K, Altorki N, Dannenberg AJ. Dihydroxy bile acids activate the transcription of cyclooxygenase-2. J Biol Chem 1998;273:2424–8.
38. Kutchera W, Jones DA, Matsunami N, Groden J, McIntyre TM, Zimmerman GA, et al. Prostaglandin H synthase 2 is expressed abnormally in human colon cancer: evidence for a transcriptional effect. Proc Natl Acad Sci USA 1996;93:4816–20.
39. von Kleist S, Chany E, Burtin P, King M, Fogh J. Immunohistology of the antigenic pattern of a continuous cell line from a human colon tumor. J Natl Cancer Inst 1975;55:555–60.
40. Knowles BB, Howe CC, Aden DP. Human hepatocellular carcinoma cell lines secrete the major plasma proteins and hepatitis B surface antigen. Science 1980;209:497–9.
41. Dignam JD, Lebovitz RM, Roeder RG. Accurate transcription initiation by RNA polymerase II in a soluble extract from isolated mammalian nuclei. Nucleic Acids Res 1983;11:1475–89.
42. Sharp PA. RNA interference—2001. Genes Dev 2001;15:485–90.
43. Kawamori T, Rao CV, Seibert K, Reddy BS. Chemopreventive activity of celecoxib, a specific cyclooxygenase-2 inhibitor, against colon carcinogenesis. Cancer Res 1998;58:409–12.
44. Glinghammar B, Inoue H, Rafter JJ. Deoxycholic acid causes DNA damage in colonic cells with subsequent induction of caspases, COX-2 promoter activity and the transcription factors NF-kB and AP-1. Carcinogenesis 2002;23:839–45.
45. Stadler J, Yeung KS, Furrer R, Marcon N, Himal HS, Bruce WR. Proliferative activity of rectal mucosa and soluble fecal bile acids in patients with normal colons and in patients with colonic polyps or cancer. Cancer Lett 1988;38:315–20.
46. Nagengast FM, Grubben MJ, van Munster IP. Role of bile acids in colorectal carcinogenesis. Eur J Cancer 1995;31A:1067–70.
47. Ohtsuka H, Abe T, Onogawa T, Kondo N, Sato T, Oshio H, et al. Farnesoid X receptor, hepatocyte nuclear factors 1alpha and 3beta are essential for transcriptional activation of the liver-specific organic anion transporter-2 gene. J Gastroenterol 2006; 41:369–77.
48. Tominaga K, Higuchi K, Sasaki E, Suto R, Watanabe T, Fujiwara Y, et al. Correlation of MAP kinases with COX-2 induction differs between MKN45 and HT29 cells. Aliment Pharmacol Ther 2004;20 Suppl 1:143–50.
49. Rudnick DA, Perlmutter DH, Muglia LJ. Prostaglandins are required for CREB activation and cellular proliferation during liver regeneration. Proc Natl Acad Sci USA 2001;98:8885–90.
50. Ionov Y, Matsui S, Cowell JK. A role for p300/CREB binding protein genes in promoting cancer progression in colon cancer cell lines with microsatellite instability. Proc Natl Acad Sci USA 2004;101:1273–8.
51. Lu Q, Hutchins AE, Doyle CM, Lundblad JR, Kwok RP. Acetylation of cAMP-responsive element-binding protein (CREB) by CREB-binding protein enhances CREB-dependent transcription. J Biol Chem 2003;278:15727–34.
52. Arany Z, Sellers WR, Livingston DM, Eckner R. E1A-associated p300 and CREB-associated CBP belong to a conserved family of coactivators. Cell 1994;77:799–800.
53. Tien ES, Davis JW, Vanden Heuvel JP. Identification of the CREB-binding protein/p300-interacting protein CITED2 as a peroxisome proliferator-activated receptor alpha coregulator. J Biol Chem 2004;279:24053–63.
54. Yoon JH, Higuchi H, Werneburg NW, Kaufmann SH, Gores GJ. Bile acids induce cyclooxygenase-2 expression via the epidermal growth factor receptor in a human cholangiocarcinoma cell line. Gastroenterology 2002;122:985–93.
55. Glinghammar B, Inoue H, Rafter JJ. Deoxycholic acid causes DNA damage in colonic cells with subsequent induction of caspases, COX-2 promoter activity and the transcription factors NF-kB and AP-1. Carcinogenesis 2002;23:839–45.

The Cerebellum
2008, 75–83

Springer

ARTICLE

Thyroid hormone transporters in the brain

TAKEHIRO SUZUKI[1,2] & TAKAAKI ABE[1]

[1]*Division of Nephrology, Endocrinology, and Vascular Medicine, Department of Medicine, Tohoku University Graduate School of Medicine, and* [2]*The 21st Century COE Program Special Research Grant from the Ministry of Education Science, Sports and Culture, Tohoku University Graduate School of Medicine, Japan*

Abstract
Thyroid hormone plays an essential role in proper mammalian development of the central nervous system and peripheral tissues. Lack of sufficient thyroid hormone results in abnormal development of virtually all organ systems, a syndrome termed cretinism. In particular, hypothyroidism in the neonatal period causes serious damage to neural cells and leads to mental retardation. Although thyroxine is the major product secreted by the thyroid follicular cells, the action of thyroid hormone is mediated mainly through the deiodination of T_4 to the biologically active form 3,3', 5-triiodo-L-thyronine, followed by the binding of T_3 to a specific nuclear receptor. Before reaching the intracellular targets, thyroid hormone must cross the plasma membrane. Because of the lipophilic nature of thyroid hormone, it was thought that they traversed the plasma membrane by simple diffusion. However, in the past decade, a membrane transport system for thyroid hormone has been postulated to exist in various tissues. Several classes of transporters, organic anion transporter polypeptide (oatp) family, Na^+/Taurocholate cotransporting polypeptide (ntcp) and amino acid transporters have been reported to transport thyroid hormones. Monocarboxylate transporter8 (MCT8) has recently been identified as an active and specific thyroid hormone transporter. Mutations in MCT8 are associated with severe X-linked psycomotor retardation and strongly elevated serum T_3 levels in young male patients. Several other molecules should be contributed to exert the role of thyroid hormone in the central nervous system.

Key words: *Thyroid hormone, transporter, organic anion transporter polypeptide, amino acid transporter, Monocarboxylate transporter, cerebellum, hypothyroidism*

Abbreviations: T_4, thyroxine; T_3, 3,3', 5-triiodo-L-thyronine; oatp, organic anion transporting polypeptide; ntcp, Na^+/taurocholate cotransporting polypeptide; MCT, monocarboxylate transporter; BBB, blood-brain barrier; CSF, cerebrospinal fluid

Introduction

Thyroid hormone is important for the development of various tissues and for the regulation of metabolic processes throughout life (1–3). In the brain, thyroid hormone regulates the process of terminal brain differentiation such as axonal and dendritic growth, synaptogenesis, neural migration and myelination (4). Therefore, thyroid hormone deficiency in the developmental period results in severe functional defects of the brain, including mental retardation, ataxia, spasticity and deafness (5). In thyroid hormone deficient rat, cells in the cortex are smaller and more closely aggregated than normal, due in part to an overall decrease in the development of axonal and dendritic processes (4). Axonal density is also decreased and the probability of axo-dendritic interaction is reduced (4). In the cerebellum, both cell migration and differentiation of granule cells are affected (2). A deficiency of myelination under hypothyroid status has been observed in the cerebral cortex, visual and auditory cortex, hippocampus and cerebellum, which were related to the observed neurodevelopmental delay (6,7).

The brain is separated from the bloodstream by the blood-brain and blood-cerebrospinal fluid (CSF) barriers, which restrict the entry of molecules into brain tissue. It has been suggested that thyroid hormone enters the brain via the blood-brain barrier (BBB) (8) or the blood-CSF barrier (9). The choroid plexus is a major component of the blood-CSF barrier, as well as the major production site of the thyroid hormone-binding protein, transthyretin. Free T_4 can cross the choroid plexus from blood to the brain (9) and one fifth of the T_4 in the brain could originate from CSF that has passed through

Correspondence: Takaaki Abe, Division of Nephrology, Endocrinology, and Vascular Medicine, Department of Medicine, Tohoku University Graduate School of Medicine, 1-1 Seiryo-cho, Aoba-ku, Sendai, 980-8574 Japan. Tel: +81 22 717 7163. Fax: +81 22 717 7168. E-mail: takaabe@mail.tains.tohoku.ac.jp

ISSN 1473-4222 print/ISSN 1473-4230 online
DOI: 10.1007/s12311-008-0029-9
Online first: 12 April 2008, ifirst: 13 August 2007

the choroid plexus (10). In the retina, the retinal pigment epithelium is the only source of transthyretin and is supposed to be a functional counterpart of choroid plexus epithelium in the blood retinal barrier (11). However, the molecular mechanisms of thyroid hormone transport in the BBB and blood-CSF barriers have not been clarified. Thyroid hormone, being hydrophobic, had been thought to enter target cell membranes by passive diffusion. However, evidence has accumulated over the past three decades for the existence of multiple thyroid hormone transporting systems in different tissues, such as liver (12–14), neuronal cells (15), pituitary (16), astrocytes (17), glial cells (18), skeletal muscles (19), red blood cells (20) and erythrocytes (21) with or without Na^+-dependency, and the *Km* values varies from the nM to μM level. Because both the action and metabolism of thyroid hormone are intracellular events, an uptake system of thyroid hormone through the plasma membrane should be required (22–24). On the contrary, transthyretin has been recognized as a major thyroid hormone binding protein in the CSF in human and rodents, its importance as a carrier for transporting T_4 into the brain was recently questioned since transthyretin deficient mice exhibit normal T_3 and T_4 concentrations in the brain parenchyma (25). These data suggest that thyroid hormone binding proteins do not represent a limiting factor for thyroid hormone to be normally distributed to the central nervous system.

Oatp1a4(oatp2) and Oatp1a5(oatp3) as thyroid hormone transporters

The characterization of thyroid hormone transport was started because of the structural and functional similarities between the choroid plexus epithelium and the retinal pigment epithelium. In 1998, Abe et al. isolated Oatp1a4(oatp2) and Oatp1a5(oatp3) from rat retina and identified them as thyroid hormone transporters (26). Hydrophobicity analyses of Oatp1a4(oatp2) and Oatp1a5(oatp3) predict 12 hydrophobic segments, which is a characteristic of various transporter families. When a *Xenopus* oocyte expression system was used, it became clear that both Oatp1a4(oatp2) and Oatp1a5(oatp3) transport T_4 and T_3. The K_m values for T_4 and T_3 by Oatp1a4(oatp2) were 6.5 μM and 5.8 μM, respectively. Oatp1a5(oatp3) also transports thyroid hormone with a K_m of 4.9 μM for T_4 and 7.3 μM for T_3. Neither Oatp1a4(oatp2)- nor Oatp1a5(oatp3)-mediated thyroid hormone uptake is dependent on extracellular Na^+. In addition, immunohistochemical analysis showed that Oatp1a4(oatp2) is localized mainly in the retinal pigment epithelium, whereas Oatp1a5(oatp3) is located in optic nerve fibers, suggesting that they might play successive roles in thyroid hormone transport in the retina and neural cells (27).

Thyroid hormone transporting OATP family in BBB and blood-CSF barrier

Subsequently, rat Oatp1a1(oatp1), which was originally identified as the bile acid transporter in the rat liver (28), also reported to transport thyroid hormone in a Na^+-independent manner (29). Localization of Oatp1a1(oatp1), and Oatp1a4(oatp2) at the apical (30) and basolateral membranes (31) of the choroid plexus epithelium was reported respectively. This spatial localization suggests the role for the oatps in the transport of thyroid hormone between the blood, CSF and brain. Recently, Oatp1a5(oatp3) expression in rat (32,33) and in mouse (34) apical membrane of choroid plexus epithelial cells was also reported. In these reports, because Oatp1a1(oatp1) expression in choroid plexus was reported to be very low or under detectable level in mRNA level (32–34), the expression of Oatp1a1(oatp1) in choroid plexus epithelial and involvement in blood-CSF barrier transportation of thyroid hormone remain to be examined. Oatp1a5(oatp3) might be another candidate for thyroid hormone transporting system in the apical side of choroid plexus epithelial cells.

In human, it was also reported that OATP1C1(OATP-F), which is highly expressed in the brain and testis, transports T_4 (*Km*=90 nM) and reverse T_3 (*Km*=128 nM) in a high affinity manner (35). In the brain, OATP-1C1(OATP-F) mRNA was detected in numerous brain regions except the pons and cerebellum (35). Immunohistochemical study revealed that OATP1C1(OATP-F) was also localized in Leydig cells of human testis, although immunohistochemical study in human brain was not performed in this report (35). The extensive expression of OATP1C1(OATP-F) throughout the brain, except for the cerebellum and pons, as well as high affinity for T_4, suggests that this transporter should be involved in the brain uptake of T_4.

The rat and mouse ortholog of human OATP1C1, Oatp1c1(oatp14) is localized preferentially in brain capillary endothelial cells capillaries in rat (36), and in mouse (37). Increased transport was demonstrated for estradiol 17-β-glucuronide, cerivastatin, troglitazone sulfate, T_4 and rT_3 in Oatp1c1(oatp14) transfected HEK293 cells. *Km* and Vmax values for these substrates show the highest affinity and specificity for T_4 and rT_3. Sugiyama and colleagues also reported the altered expression level of Oatp1c1(oatp14) in isolated brain capillaries in hypothyroid and hyperthyroid rat models (36). In hypothyroid rats, Oatp1c1 mRNA and protein are up-regulated, whereas in hyperthyroid rats the expression of Oatp1c1(oatp14) is down-regulated. Thus, the thyroid state-dependent regulation of

Oatp1c1(oatp14) counteracts the effects of alternations in circulating T_4 levels on brain T_4 uptake. Recently, Bronger H. et al. reported that they detected OATP1A2(OATPA) expression in the apical membrane of endothelial cells of the BBB by immunofluorescence microscopy (38). On the other hand, no significant immunostaining was observed for OATP1C1(OATP-F) in human brain samples. So OATP1C1(OATP-F) localization in human BBB is still controversial. OATP1A2(OATP-A) was reported that it transport T_3 (K_m=6.5 μM) and T_4 (K_m=8.0 μM) (39) and is expressed exclusively in the brain (40). OATP1A2(OATAP-A) might be also a component of the hormone transporting system in human BBB.

Classification of the organic anion transporter family

The organic anion transporter comprises a large family of Na^+-independent transporters (Table I, Figure 1). Of the known rat organic anion transporters, Oatp1a1(oatp1) (29), Oatp1a4(oatp2) (26), Oatp1a5(oatp3) (26), Oatp4a1(oatp-E) (39), Oatp1c1(otap14) (36), Oatp6b1(GST-1/oatp16) and Oatp6c1(GST-2/oatp18) (41), and Oatp4c1-(oatp-R) (42), have been reported to transport thyroid hormone. The tissue distribution of the rat oatp family is rather broad except for gonad specific Oatp6b1(GST-1/oatp16) and Oatp6c1(GST-2/oatp18), or Oatp4c1 Oatp4c1(oatp-R), which is exclusively expressed in kidney (Table I). The phylogenetic tree for organic anion transporters is shown in Figure 1. The complicated nomenclature represents another difficulty in characterizing the oatp family. In the beginning, the oatp family was given the Gene Symbol of solute carrier family21 (SLC21) by the HUGO Gene Nomenclature Committee. Recently, the HUGO Gene Nomenclature Committee adopted a new nomenclature, SLCO (character 'O' is from the head letter of OATP) (Table I, Figure 1). According to the SLCO nomenclature, for instance, LST-1/OATP-C/OAT-P2(OATP1B1) and LST-2/OATP8(OATP1B3) are named *SLCO1B1* and *SLCO1B3*, respectively (see Table I).

Several oatps are involved in thyroid hormone transport in humans

Compared with rat oatps, the expression patterns of human organic anion transporters are more tissue specific. Human OATP1A2(OATPA), which transports T_3 (K_m=6.5 μM) and T_4 (K_m=8.0 μM) (39), is expressed exclusively in the brain (40). Human liver-specific transporters OATP1B1(LST-1/OATP-C/OATP2) (40,43–45) and OATP1B3(LST-2/OATP8) (46,47), which transport thyroid hormone,

Table I. Organic anion transporter polypeptides.

Protein name	Gene symbol	Novel protein name	Novel gene symbol	expression	reference
Human OATP					
PGT	*SLC21A2*	OATP2A1	*SLCO2A1*	widely	74
OATP-A	*SLC21A3*	OATP1A2	*SLCO1A2*	brain	39,40,75
LST-1/OATP-C/OATP2	*SLC21A6*	OATP1B1	*SLCO1B1*	liver only	40,43,44,45
LST-2/OATP8	*SLC21A8*	OATP1B3	*SLCO1B3*	liver only	46,47
OATP-B/MOAT1	*SLC21A9*	OATP2B1	*SLCO2B1*	widely	45
OATP-D	*SLC21A11*	OATP3A1	*SLCO3A1*	widely	76
OATP-E	*SLC21A12*	OATP4A1	*SLCO4A1*	widely	39,54
OATP-F	*SLC21A14*	OATP1C1	*SLCO1C1*	brain, testis	35
OATP-J/OATP-RP4	*SLC21A15*	OATP5A1	*SLCO5A1*	?	
GST/OATP-I	*SLC21A19*	OATP6A1	*SLCO6A1*	testis	41
OATP-R	*SLC21A20*	OATP4C1	*SLCO4C1*	kidney	42
Rat oatp					
oatp1	*slc21a1*	Oatp1a1	*Slco1a1*	liver, kidney	28,29
rPGT	*slc21a2*	Oatp2a1	*Slco2a1*	widely	77
OAT-K1 OAT-K2	*slc21a4*	Oatp1a3-v1 Oatp1a3-v2	*Slco1a3*	kidney	78,79
oatp2	*slc21a5*	Oatp1a4	*Slco1a4*	retina, liver brain	26,80
oatp3	*slc21a7*	Oatp1a5	*Slco1a5*	retina, brain liver, kidney	26
oatp4/rlst-1	*slc21a9*	Oatp1b2	*Slco1b2*	liver only	81,82
moat1/oatp-B	*slc21a10*	Oatp2b1	*Slco2b1*	widely	83
oatp-D	*slc21a11*	Oatp3a1	*Slco3a1*	widely	76
oatp-E	*slc21a12*	Oatp4a1	*Slco4a1*	widely	39
oatp5	*slc21a13*	Oatp1a6	*Slco1a6*	kidney	84
oatp14	*slc21a14*	Oatp1c1	*Slco1c1*	brain	36
rGST-1/oatp16	*slc21a16*	Oatp6b1	*Slco6b1*	testis	41
rGST-2/oatp18	*slc21a18*	Oatp6c1	*Slco6c1*	testis	41
oatp-R	*slc21a20*	Oatp4c1	*Slco4c1*	kidney	42

Nomenclature of the organic anion transporter polypeptide family

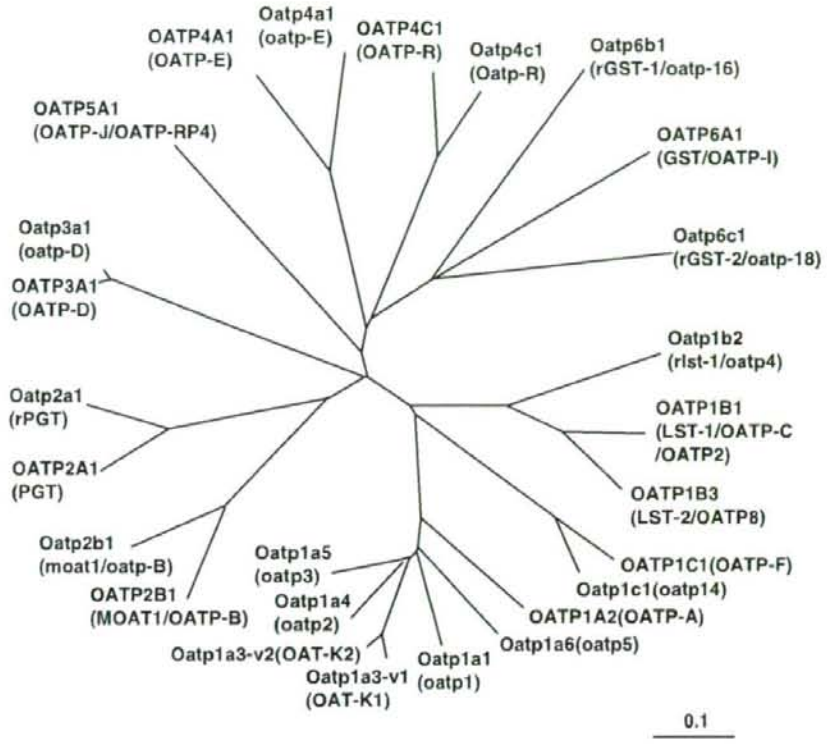

Figure 1. The phylogenetic relationships between members of the organic anion transporter polypeptide family. Branch lengths are drawn to scale.

are exclusively expressed in the liver. OATP1B1-(LST-1) transports thyroid hormone with a K_m of 3.0 μM for T_4 and 2.7 μM for T_3. The K_m values for T_4 and T_3 of OATP1B3 (LST-2) are 6.5 μM and 5.9 μM, respectively. Human OATP4A1(OATP-E) transports thyroid hormone in a Na^+-independent manner, and the K_m value for T_3 is 0.9 μM, which is the lowest value among the oatp family (39). OATP4A1(OATP-E) is expressed abundantly in various peripheral tissues, as well as in the small intestine.

It is well known that study of the OATP family had started from the research of the bile acid uptake in the liver (48). After biosynthesis from the cholesterol in the hepatocyte, bile acid is excreted in the bile duct and this secreted bile acid in the alimentary canal is re-absorbed from the digestive tract and re-entered to the blood. This circulating bile acid is re-uptaked by liver cells. Those processes are called enterohepatic circulation (48). The first member of organic anion transporter family identified in the rat liver was Oatp1a1(oatp1), the Na^+-independent organic anion transporting polypeptide, transports bile acid, bromosulfophthalein, as well as conjugated and unconjugated steroid hormones from the blood stream into hepatocytes (28) and also transports thyroid hormone (29). Physiological studies have suggested the presence of other members of this family in the liver. Subsequently, Oatp1a4(oatp2) and Oatp1a5(oatp3) in rat, OATP1B1(LST-1/OATP-C/OATP2) and OATP1-B3(LST-2/OATP8) in human are identified as bile acid transporters.

The enterohepatic circulation of thyroid hormone has also already been well established in rat (49,50). Because OATP4A1(OATP-E), OATP1B1(LST-1/OATP-C/OATP2), and OATP1B3(LST-2/OAT-P8) transport both thyroid hormone and taurocholate, it is suggested that, in human, OATP4-A1(OATP-E), OATP1B1(LST-1/OATP-C/OAT-P2), and OATP1B3(LST-2/OATP8) might be involved in the transport of bile acids and thyroid hormone in the enterohepatic circulation. These data suggest the possibility that molecules, which transport bile acid, also transport thyroid hormone *in vivo*.

Rat gonad-specific organic anion transporter Oatp6b1(GST-1) and Oatp6c1(GST-2) have been isolated and are abundantly expressed in testis and moderately in ovary, adrenal gland and epididymis (41). Both Oatp6b1(GST-1) and Oatp6c1(GCT-2) are members of the oatp family and are reported to

transport T_4 with K_m of 6.4 μM and 5.8 μM, respectively. The human counterpart, human GST, was also isolated and is exclusively expressed in the testis (41). Because hypothyroidism in neonatal and early infantile periods impairs the development and maturation of gonads and causes infertility in adults, those gonad-specific transporters might be involved in the regulation of the development and function of gonads.

In the kidney, kidney specific organic anion transporter OATP4C1(OATP-R) and its rat counterpart Oatp4c1(oatp-R) have been isolated and proven to transport both T_3 and T_4 (42). The K_m values for T_3 of human OATP4C1 and rat Oatp4c1 are 5.9 μM and 1.9 μM, respectively. Immunohistochemistry revealed that rat Oatp4c1(oatp-R) was expressed in the proximal tubules and so far no other OATP family member that transports thyroid hormone was found to be expressed in human kidney. In addition, the proximal tubule cells express type1 5'-deiodinase, which is a major enzyme catalyzing the conversion of T_3 from T_4 (51). Colocalization of Oatp4c1 and type1 5'-deiodinase might be functionally concerned in the regulation of thyroid hormone metabolism in the proximal tubules.

Monocarboxylate transporter family

The MCT(SLC16) family is named because the first 4 members have been characterized as transporters of monocarboxylates such as lactate, pyruvate, and ketone bodies (52). To date, 14 members of the MCT family have been identified in various tissues from different species. However, the types of ligands have been identified for only six members (i.e., monocarboxylates for MCT1-4 and aromatic amino acid derivatives for MCT8 and MCT10). The functions of the other MCT families remain to be determined. The MCTs are proteins of 426–565 amino acids with 12 predicted transmembrane domains. Among MCTs, MCT8 is expressed in many tissues, including human liver, kidney, heart, brain, placenta, lung and skeletal muscle (53). Recently, Friesema et al. identified rat MCT8 as a specific thyroid hormone transporter (53). MCT8-expressing in *Xenopus* oocytes showed the uptake of T_4, T_3, rT_3 and 3,3'-T_2, and the *Km* values of 4.7 μM for T_4, 4.0 μM for T_3, and 2.2 μM for rT_3, which was at an order lower than for the isolated other thyroid hormone transporters. This transport of T_3 by MCT8 is Na^+-independent, although T_4 transport is decreased in the absence of Na^+ (53). In mouse central nervous system, the highest mRNA expression levels of MCT8 were detected in neuronal cells of the cerebrocortex, olfactory bulb, hippocampus, amygdala, moderate levels in the striatum and cerebellum, and low levels in some neuroendocrine nuclei (54). These neural cell populations are thyroid hormone-sensitive and the thyroid hormone transport system in those neural tissues might be mediated by MCT8.

The pathophysiological relevance of MCT8 as a thyroid hormone transporter has been reported in patients with a novel syndrome of severe X-linked mental retardation and psychomotor disability and strongly elevated T_3 levels and low T_4 (55,56,also reviewed in 57,58). This severe phenotype is explained partly by the recent reports that MCT8 is expressed specifically in thyroid hormone sensitive neuronal populations (54,59,60). MCT8 might be important for the neuronal uptake of T_3 produced from T_4 in neighboring astrocytes that express type2 iodothyronine deiodinase, which catalyzes the conversion of T_3 from T_4 (61).

Two research groups have recently reported MCT8 deficient mice (62,63). MCT8 deficient mice show disturbed profiles of serum thyroid hormone levels, high concentration of serum T_3 and low serum T_4 level, however there was no obvious phenotype of developmental retardation in nervous system (62,63). The fact that the neurological manifestations present in MCT8-deficiet human have not been replicated in the mouse model might be due to species-specific regulation of intracellular thyroid hormone availability or demands of thyroid hormone for normal function in central nervous system.

Uptake of T_3 into the brain was almost absent in MCT8-null mice, suggests that MCT8 is a key molecule in T_3 transverse into the brain (62,63). Whereas, entry of T_4 into the brain was not changed in the absence of MCT8 (63), indicates the presence of other thyroid hormone transporters such as Oatp1c1(oatp14) at the blood brain barrier that which carry T_4 into the tissues (37). Trajkovic et al. reported that there was no obvious morphological abnormality of Purkinje cells and the external granule cell layer in the cerebellum of the 12-day-old MCT8-deficiet mice compared to control animals (63). Purkinje cell cultures from both neonatal MCT8-null and wild type mice demonstrated the similar normal neuronal sensitivity (increased dendritic parameters) to T_3 treatment *in vitro* (63), implies the neuronal MCT8 deficiency might be compensated for by other thyroid hormone transporters in mice, and MCT8-null mice are protected from the neurological deficit observed in humans.

Amino acid transporter is member of thyroid hormone transporter family

Amino acids, especially essential amino acids, are required for protein synthesis and as energy sources in all living cells. Because most amino acids are hydrophilic, they require special membrane transport

systems to penetrate the cell membrane. Many amino acid transporters, each of which have 12 transmembrane regions, have been characterized (64). In addition, the cell-surface glycoprotein 4F2 heavy chain (4F2hc; CD98 in mouse) has also been identified as being part of an amino acid transporter. 4F2hc has a single transmembrane domain and a 120-kDa disulfide-linked protein formed by a heteromeric glycosylated 40 kDa light chain together with an 80 kDa heavy chain (65,66). The expression of 4F2hc in *Xenopus* oocytes induces low levels of cysteine, dibasic and neutral amino acid transport (67). Friesema et al. (68) reported that co-injection of cRNAs for 4F2hc and human LAT1 light chain not only transported amino acids (Phe, Tyr, Leu and Trp), which is a characteristic of the system L amino acid transporter (a Na^+-independent exchange of large, neutral amino acids), but also transported thyroid hormone in a Na^+-independent manner. The K_m values for T_4, T_3, reverse T_3 and T_2 were 7.9 μM, 0.8 μM, 12.5 μM and 7.9 μM, respectively. Bloundeau et al. (69) showed that aromatic and neutral amino acids are transported into cultured astrocytes via the Na^+-independent system L_y which is related to the thyroid hormone transport system. These data suggest the contribution of the amino acid transporter LAT-1/4F2hc complex to thyroid hormone transport in astrocytes.

Differences of K_m values and Na^+ dependency

Several questions arise from recent work on the identification of thyroid hormone transporters, the most common being why are there different K_m values between cDNA expression systems and *in vitro* culture systems? The *in vitro* studies characterized two saturable sites for thyroid hormone binding; one is characterized by high affinity and low capacity, and the other by low affinity and high capacity (12,24). The high-affinity uptake of T_3 is mostly in the nM range and is often energy and extracellular Na^+ dependent. However, in the low-affinity uptake process the K_m for T_4 and T_3 of the fraction is in the μM range, which is similar to that of oatps and amino acid transporters expressed in *Xenopus* oocytes (68), hepatocytes (13) and glial cells (18). Little is known about the molecular entity responsible for the high affinity-system, except OATP1C1(OATP-F) and Oatp1c1(oatp14), although differences in the types of assays or experimental procedures used are possible explanations for the discrepant results.

Another controversy arises from the fact that the oatp family- and amino acid transporter-mediated uptake of thyroid hormone is not dependent on extracellular Na^+ *in vitro*, whereas the transporting mechanisms of thyroid hormones in the tissues are heterogeneous in terms of Na^+ dependency: Na^+-dependent (13), Na^+-independent (14,19), and mixed (18,20). Rat ntcp was reported to transport thyroid hormone (29). Ntcp consists of ~350 amino acids with seven putative trans-membrane domains (70). Ntcp is expressed only in the basolateral cell membrane of hepatocytes and is the major transporting mechanism for conjugated bile acids, especially taurocholate, into the liver (other bile acids are mainly transported by oatps) (71). The Na^+-independent fraction of thyroid hormone uptake into the tissues could be partly attributed to the oatp family and 4F2c-L-type amino acid transporter complex. However, the molecular entities responsible for the Na^+-dependent system in various tissues are still unclear, because the Na^+-dependent transporters, ntcp and ASBT, are not expressed widely (71). There might be several other candidate molecules that are responsible for transporting thyroid hormone.

Thyroid hormone transport-related diseases

Certain individuals exhibit a syndrome of resistance to thyroid hormone in many tissues. Such patients have reduced clinical and biochemical manifestations thyroid hormone action relative to the circulating hormone level (Refetoff's syndrome) (72,73). In practice, most patients are identified by the persistent elevation of serum levels of T_4 and T_3 with inappropriately non-suppressed TSH, in the absence of intercurrent acute illness, drugs, or alteration of thyroid hormone binding to serum proteins. One well-known molecular basis is an abnormality of the nuclear thyroid hormone receptor (73). However, other functional defects in such patients have also been postulated (72). One possible mechanism is reduced hormone availability to tissues because of impaired thyroid hormone entry into target cells. Thus, the finding of a thyroid hormone transporter might provide a clue for identifying the genetic basis for the lack of thyroid hormone responsiveness.

References

1. Porterfield SP, Hendrich CE. The role of thyroid hormones in prenatal and neonatal neurological development-current perspectives. Endocr Rev. 1993;14:94–106.
2. Oppenheimer JH, Schwartz HL. Molecular basis of thyroid hormone-dependent brain development. Endocr Rev. 1997;18:462–75.
3. Yen PM. Physiological and molecular basis of thyroid hormone action. Physiol Rev. 2001;81:1097–142.
4. Eayrs JT. Influence of the thyroid on the central nervous system. Br Med Bull. 1960;16:122–7.
5. Thompson CC, Potter GB. Thyroid hormone action in neural development. Cerebral Cortex. 2000;10:939–45.
6. Balazs R, Brooksbank BW, Davison AN, Eayrs JT, Wilson DA. The effect of neonatal thyroidectomy on myelination in the rat brain. Brain Res. 1969;15:219–32.
7. Balazs R, Kovacs S, Cocks WA, Johnson AL, Eayrs JT. Effect of thyroid hormone on the biochemical maturation of rat brain: Postnatal cell formation. Brain Res. 1971;25:555–70.

8. Pardridge WM. Targeted delivery of hormones to tissues by plasma proteins. In: Conn M, editor. Handbook of physiology; Section 7: The Endocrine System, Vol. I: Cellular endocrinology. Oxford: Oxford University Press; 335–82.
9. Southwell BR, Duan W, Alcorn D, Brack C, Richardson SJ, Kohrle J, et al. Thyroxine transport to the brain: Role of protein synthesis by the choroid plexus. Endocrinology. 1993;133:2116–26.
10. Chanoie JP, Akex S, Fang SL, Stone S, Leonard JL, Korhle J, et al. Role of transthyretin in the transport of thyroxine from the blood to the choroid plexus, the cerebrospinal fluid, and the brain. Endocrinology. 1992;130:933–8.
11. Cavallaro T, Martone RL, Dwork AJ, Schon EA, Herbert J. The retinal pigment epithelium is the unique site of transthyretin synthesis in the rat eye. Invest Ophthalmol Vis Sci. 1990;31:497–501.
12. Krenning E, Docter R, Bernard B, Visser T, Hennemann G. Characteristics of active transport of thyroid hormone into rat hepatocytes. Biochim Biophys Acta. 1981;676:314–20.
13. Blondeau J-P, Osty J, Francon J. Characterization of the thyroid hormone transport system of isolated hepatocytes. J Biol Chem. 1988;263:2685–92.
14. Topliss DJ, Kolliniatis E, Barlow JW, Lim CF, Stockigt JR. Uptake of 3,5,3'-triiodothyronine by cultured rat hepatoma cells is inhibitable by nonbile acid cholephils, diphenylhydantoin, and nonsteroidal anti-inflammatory drugs. Endocrinology. 1989;124:980–6.
15. Chantoux F, Blondeau JP, Francon J. Characterization of the thyroid hormone transport system of cerebrocortical rat neurons in primary culture. J Neurochem. 1995;65:2549–54.
16. Gingrich SA, Smith PJ, Shapiro LE, Surks MI. 5,5'-Diphenylhydantoin (phenytoin) attenuates the action of 3,5,3'- triiodo-L-thyronine in cultured GC cells. Endocrinology. 1985;116:2306–13.
17. Beslin A, Chantoux F, Blondeau J-P, Francon J. Relationship between the thyroid hormone transport system and the Na^+-H^+ exchanger in cultured rat brain astrocytes. Endocrinology. 1995;136:5385–90.
18. Francon J, Chantoux F, Blondeau JP. Carrier-mediated transport of thyroid hormones into rat glial cells in primary culture. J Neurochem. 1989;53:1456–3.
19. Centanni M, Robbins J. Role of sodium in thyroid hormone uptake by rat skeletal muscle. J Clin Invest. 1987;80: 1068–72.
20. Galton VA, St Germain DL, Whittemore S. Cellular uptake of 3,5,3'-triiodothyronine and thyroxine by red blood and thymus cells. Endocrinology. 1986;118:1918–23.
21. Osty J, Jego L, Francon J, Blondeau J-P. Characterization of triiodothyronine transport and accumulation in rat erythrocytes. Endocrinology. 1988;123:2303–11.
22. Abe T, Suzuki T, Unno M, Tokui T, Ito S. Thyroid hormone transporters: Recent advances. Trends Endocrinol Metab. 2002;13:215–20.
23. Friesema EC, Jansen J, Milici C, Visser TJ. Thyroid hormone transporters. Vitam Horm. 2005;70:137–67.
24. Hennemann G, Docter R, Friesema EC, de Jong M, Krenning EP, Visser TJ. Plasma membrane transport of thyroid hormones and its role in thyroid hormone metabolism and bioavailability. Endocr Rev. 2001;22:451–76.
25. Palha JA, Fernandes R, de Escobar GM, Episkopou V, Gottesman M, Saraiva MJ, Gottesman ME, Saraiva MJ. Transthyretin regulates thyroid hormone levels in the choroid plexus, but not in the brain parenchyma: Study in a transthyretin-null mouse model. Endocrinology. 2000;141: 3267–72.
26. Abe T, Kakyo M, Sakagami H, Tokui T, Nishio T, Tanemoto M, et al. Molecular characterization and tissue distribution of a new organic anion transporter subtype (oatp3) that transports thyroid hormones and taurocholate and comparison with oatp2. J Biol Chem. 1998;273: 22395–401.
27. Ito A, Yamaguchi K, Onogawa T, Unno M, Suzuki T, Nishio T, et al. Distribution of organic anion transporting polypeptide2 (oatp2) and oatp3 in rat retina. Invest Ophthalmol Vis Sci. 2002;43:58–63.
28. Jacquemin E, Hagenbuch B, Stieger B, Wolkoff AW, Meier PJ. Expression cloning of a rat liver Na^+- independent organic anion transporter. Proc Natl Acad Sci USA. 1994;91:133–7.
29. Friesema ECH, Doctera R, Moeringsa EPCM, Stiegerb B, Hagenbuch B, Meier PJ, et al. Identification of thyroid hormone transporters. Biochem Biophys Res Commun. 1999;254:497–501.
30. Angeletti RH, Novikoff PM, Juvvadi SR, Fritschy JM, Meier PJ, Wolkoff AW. The choroid plexus epithelium is the site of the organic anion transport protein in the brain. Proc Natl Acad Sci USA. 1997;94:283–6.
31. Gao B, Stieger B, Noé B, Fritschy JM, Meier PJ. Locaization of the organic anion transporting polypeptides 2(Oatp2) in capillary endothelium and choroids plexus epithelium of rat brain. J Histochem Cytochem. 1999;47:1255–64.
32. Ohtsuki S, Takizawa T, Takanaga H, Terasaki N, Kitazawa T, Sasaki M, et al. *In vitro* study of functional expression organic anion transporting polypeptide 3 at rat choroid plexus epithelial cells and its involvement in the cerebrospinal fluid-to-blood transport of estrone-3-sulfate. Mol Phramacol. 2003;63:532–7.
33. Kusuhara H, He Z, Nagata Y, Nozaki Y, Ito T, Masuda H, et al. Expression and functional involvement of organic anion transporting polypeptide subtype 3 (*Slc2a7*) in rat choroids plexus. Phram Res. 2003;20:720–7.
34. Ohtsuki S, Takizawa T, Takanaga H, Hori S, Hosoya K, Terasaki T. Localization of organic anion transporting polypeptide 3(oatp3) in mouse brain parencymal and capillary endothelial cell. J Neurochem. 2004;90:743–9.
35. Pizzagalli F, Hagenbuch B, Stieger B, Klenk U, Folkers G, Meier PJ. Identification of a novel human organic anion transporting polypeptide as a high affinity thyroxine transporter. Mol Endocrinol. 2002;16:2283–96.
36. Sugiyama D, Kusuhara H, Taniguchi H, Ishikawa S, Nozaki Y, Aburatani H, et al. Functional characterization of rat brain-specific organic anion Transporter (Oatp14) at the blood-brain barrier: High affinity transporter for thyroxine. J Biol Chem. 2003;278:43489–95.
37. Tohyama K, Kusuhara H, Sugiyama Y. Involvement of mutispecific organic anion transporter, Oatp14 (*Slc21a14*), in the transport of thyroxine across the blood-brain barrier. Endocrinology. 2004;145:4384–91.
38. Bronger H, Konig J, Kopplow K, Steiner H-H, Ahmadi R, Herold-Mende C, et al. ABCC drug efflux pumps and organic anion uptake transporters in human gliomas and the blood-tumor barrier. Cancer Res. 2005;65:11419–28.
39. Fujiwara K, Adachi H, Nishio T, Unno M, Tokui T, Okabe M, et al. Identification of thyroid hormone transporters in humans: Different molecules are involved in a tissue-specific manner. Endocrinology. 2001;142:2005–12.
40. Abe T, Kakyo M, Tokui T, Nakagomi R, Nishio T, Nakai D, et al. Identification of a novel gene family encoding human liver-specific organic anion transporter LST-1. J Biol Chem. 1999;274:17159–63.
41. Suzuki T, Onogawa T, Asano N, Mizutamari H, Mikkaichi T, Tanemoto M. Identification and characterization of novel rat and human gonad-specific organic anion transporters. Mol Endocrinol. 2003;17:1203–15.
42. Mikkaichi T, Suzuki T, Onogawa T, Tanemoto M, Mizutamari H, Okada M, et al. Isolation and characterization of a digoxin transporter and its rat homologue expressed in the kidney. Proc Natl Acad Sci USA. 2004;101:3569–74.
43. Hsiang B, Zhu Y, Wang Z, Wu Y, Sasseville V, Yang W-P, et al. A novel human hepatic organic anion transporting polypeptide (OATP2). Identification of a liver-specific human organic

anion transporting polypeptide and identification of rat and human hydroxymethylglutaryl-CoA reductase inhibitor transporters. J Biol Chem. 1999;274:37161–8.
44. Kõnig J, Cui Y, Nies AT, Keppler D. A novel human organic anion transporting polypeptide localized to the basolateral hepatocyte membrane. Am J Physiol. 2000;278:G156–64.
45. Tamai I, Nezuc J-I, Uchinob H, Saib Y, Okuc A, Shimane M, et al. Molecular identification and characterization of novel members of the human organic anion transporter (OATP) family. Biochem Biophys Res Commun. 2000;273:251–60.
46. Abe T, Unno M, Onogawa T, Tokui T, Kondo N, Nakagomi R, et al. LST-2, a human liver-specific organic anion transporter, determines methotrexate sensitivity in gastrointestinal cancers. Gastroenterology. 2001;120: 1689–99.
47. Konig J, Cui Y, Nies AT, Keppler D. Localization and genomic organization of a new hepatocellular organic anion transporting polypeptide. J Biol Chem. 2000;275:23161–8.
48. Meier PJ, Stieger B. Bile salt transporters. Annu Rev Physiol. 2002;64:635–61.
49. Albert A, Keating FR. The role of the gastrointestinal tract, including the liver, in the metabolism of radiothyroxine. Endocrinology. 1952;51:427–43.
50. DiStefano JJ.III, Nguyen TT, Yen Y-M. Sites and patterns of absorption of 3,5,3'-triiodothyronine and thyroxine along rat small and large intestines. Endocrinology. 1992;131:275–80.
51. Lee WS, Berry MJ, Hediger MA, Larsen PR. The type 1 iodothyronine 5'-deiodinase messenger ribonucleic acid is localized to the S3 segment of the rat kidney proximal tubule. Endocrinology. 1993;132:2136–40.
52. Halestrap1 AP, Meredith D. The SLC16 gene family: from monocarboxylate transporters (MCTs) to aromatic amino acid transporters and beyond. Pflugers Arch. 2004;447:619–28.
53. Friesema EC, Ganguly S, Abdalla A, Manning Fox JE, Halestrap AP, Visser TJ. Identification of monocarboxylate transporter 8 as a specific thyroid hormone transporter. J Biol Chem. 2003;278:40128–35.
54. Heuer H, Maier MK, Iden S, Mittag J, Friesema EC, Visser TJ, et al. The monocarboxylate transporter 8 linked to human psychomotor retardation is highly expressed in thyroid hormone-sensitive neuron populations. Endocrinology. 2005;146:1701–6.
55. Friesema EC, Grueters A, Biebermann H, Krude H, von Moers A, Reeser M, et al. Association between mutations in a thyroid hormone transporter and severe X-linked psychomotor retardation. Lancet. 2004;364:1435–7.
56. Dumitrescu AM, Liao XH, Best TB, Brockmann K, Refetoff S. A novel syndrome combining thyroid and neurological abnormalities is associated with mutations in a monocarboxylate transporter gene. Am J Hum Genet. 2004;74:168–75.
57. Jansen J, Friesema EC, Milici C, Visser TJ. Thyroid hormone transporters in health and disease. Thyroid. 2005;15:757–68.
58. Friesema EC, Jansen J, Heuer H, Trajkovic M, Bauer K, Visser TJ. Mechanisms of disease: Psychomotor retardation and high T3 levels caused by mutations in monocarboxylate transporter 8. Nat Clin Pract Endocrinol Metab. 2006;2:512–23.
59. Alkemade A, Friesema EC, Unmehopa UA, Fabriek BO, Kuiper GG, Leonard JL, et al. Neuroanatomical pathway for thyroid hormone feed back in the human hypothalamus. J Clin Enodocinol Metab. 2005;90:4322–34.
60. Alkemade A, Friesema EC, Kuioer GG, Wiersinga WM, Swaab DF, Visser TJ, et al. Novel neuroanatomical pathways for thyroid hormone action in the human anterior pituitary. Eur J Endocrinol. 2006;154:491–500.
61. Guandano-Ferraz A, Obregon MJ, Germain DLS, Bernal J. The type 2 iodothyronine deiodinase is expressed primarily in glial cells in the neonatal rat brain. Proc Natl Acad Sci USA. 1997;94:10391–6.
62. Dumitrescu AM, Liao X-H, Weiss RE, Millen K, Refetoff S. Tissue-specific thyroid hormone deprivation and excess in monocarboxylate transporter (Mct) 8-deficient mice. Endocrinology. 2006;147:4036–43.
63. Trajkovic M, Visser TJ, Mittag J, Horn S, Lukas J, Darras VM, et al. Abnormal thyroid hormone metabolism in mice lacking the monocarboxylate transporter 8. J Clin Invest. 2007;117:627–35.
64. Malandro MS, Kilberg MS. Molecular biology of mammalian amino acid transporters. Annu Rev Biochem. 1996;65:305–36.
65. Haynes BF, Hemler ME, Mann DL, Eisenbarth GS, Shelhamer J, Mostowski HS, et al. Characterization of a monoclonal antibody (4F2) that binds to human monocytes and to a subset of activated lymphocytes. J Immunol. 1981;126:409–14.
66. Mastroberardino L, Spindler B, Pfeiffer R, Skelly PJ, Loffing J, Shoemaker CB, et al. Amino-acid transport by heterodimers of 4F2hc/CD98 and members of a permease family. Nature. 1998;95:288–91.
67. Wells RG, Lee W-S, Kanai Y, Leiden JM, Hediger MA. The 4F2 antigen heavy chain induces uptake of neutral and dibasic amino acids in *Xenopus* oocytes. J Biol Chem. 1992;267:15285–88.
68. Friesema ECH, Docter R, Moerings EPCM, Verrey F, Krenning EP, Hennemann G, et al. Thyroid hormone transport by the heteromeric human system L amino acid transporter. Endocrinology. 2001;142:4339–48.
69. Blondeau JP, Beslin A, Chantoux F, Francon J. Triiodothyronine is a high-affinity inhibitor of amino acid transport system L1 in cultured astrocytes. J Neurochem. 1993;60:1407–13.
70. Hagenbuch B, Stieger B, Foguet M, Lubbert H, Meier PJ. Functional expression cloning and characterization of the hepatocyte Na^+/bile acid cotransport system. Proc Natl Acad Sci USA. 1991;88:10629–33.
71. Hagenbuch B, Dawson P. The sodium bile salt cotransport family SLC10. Pflugers Arch. 2004;447:566–70.
72. Refetoff S, Weiss RE, Usala SJ. The syndromes of resistance to thyroid hormone. Endocr Rev. 1993;14:348–99.
73. Yen PM. Molecular basis of resistance to thyroid hormone. Trends Endocrinol Meatb. 2003;14:327–33.
74. Lu R, Kanai N, Shuster VL. Cloning *in vitro* expression, and tissue distribution of a human prostaglandin transporter cDNA (hPGT). J Clin Invest. 1996;98:1142–9.
75. Kullak-Ublick GA, Hagenbuch B, Stieger B, Schteingart CD, Hofmann AF, Wolkoff AW, et al. Molecular and functional characterization of an organic anion transporting polypeptide cloned from human liver. Gastroenterology. 1995;109:1274–82.
76. Adachi H, Suzuki T, Abe M, Asano N, Mizutamari H, Tanemoto M, et al. Molecular characterization of human and rat organic anion transporter OATP-D. Am J Physiol. 2003;285:F1188–97.
77. Kanai N, Lu R, Satriano JA, Bao Y, Wolkoff AW, Schuster VL. Identification and characterization of a prostaglandin transporter. Science. 1995;268:866–9.
78. Saito H, Masuda S, Inui KI, Saito H, et al. Cloning and functional characterization of a novel rat organic anion transporter mediating basolateral uptake of methotrexate in the kidney. J Biol Chem. 1996;271:20719–25.
79. Masuda S, Ibaramoto K, Takeuchi A, Saito H, Hashimoto Y, Inui K, et al. Cloning and functional characterization of a new multispecific organic anion transporter, OAT-K2, in rat kidney. Mol Pharmacol. 1999;55:743–52.
80. Noé B, Hagenbuch B, Stieger B, Meier PJ. Isolation of a multispecific organic anion and cardiac glycoside transporter from rat. Proc Natl Acad Sci USA. 1997;94:10346–50.
81. Kakyo M, Unno M, Tokui T, Nakagomi R, Nishio T, Iwasashi H, et al. Molecular characterization and functional regulation of a novel rat liver-specific organic anion transporter rlst-1. Gastroenterology. 1999;117:770–5.

82. Cattori V, Hagenbucha B, Hagenbucha N, Stiegera B, Hac R, Winterhalterb KE, et al. Identification of organic anion transporting polypeptide 4 (Oatp4) as a major full-length isoform of the liver-specific transporter-1 (rlst-1) in rat liver. FEBS Lett. 2000;474:242–5.
83. Nishio T, Adachi F, Nakagomi R, Tokui T, Sato E, Tanemoto M, Fujiwara K, at al, Molecular identification of a rat novel organic anion transporter moat1, which transports prostaglandin D(2), leukotriene C(4), and taurocholate. Biochem Biophys Res Commun. 2000;275:831–8.
84. Choudhuri S, Ogura K, Klaassen CD. Cloning, expression, and ontogeny of mouse organic anion-transporting polypeptide-5, a kidney-specific organic anion transporter. Biochem Biophys Res Commun. 2001;280:92–8.

THE JOURNAL OF BIOLOGICAL CHEMISTRY VOL. 283, NO. 18, pp. 12241–12247, May 2, 2008

MAGI-1a Functions as a Scaffolding Protein for the Distal Renal Tubular Basolateral K^+ Channels*[S]

Received for publication, September 14, 2007, and in revised form, February 7, 2008 Published, JBC Papers in Press, February 26, 2008, DOI 10.1074/jbc.M707738200

Masayuki Tanemoto[1], Takafumi Toyohara, Takaaki Abe, and Sadayoshi Ito

From the Division of Nephrology, Hypertension, and Endocrinology, Department of Medicine, Tohoku University Graduate School of Medicine, Sendai, Miyagi 980-857, Japan

As the K^+ recycling pathway for renal Na^+ reabsorption, renal tubular K^+ channels participate in the fluid and electrolyte homeostasis. Previously, we showed that the Kir5.1/Kir4.1 heteromer, which is a heteromeric assembly of two inwardly rectifying K^+ channels, composes the principal basolateral K^+ channels in distal renal tubules and that two motifs in the carboxyl-terminal portion of the Kir4.1 subunit regulate its functional expression. In this study, by using yeast two-hybrid screening, we identified a new isoform of membrane-associated guanylate kinase with inverted domain structure 1 (MAGI-1a-long) as a scaffolding protein for the basolateral K^+ channels. MAGI-1a-long interacted with the PSD-95/Dlg/ZO-1 (PDZ)-binding motif of Kir4.1 by its fifth PDZ domain, and a high salt diet, which could suppress mineralocorticoid secretion, facilitated the interaction. The phosphorylation of serine 377 in the PDZ-binding motif disrupted the interaction, and the disruption of the interaction altered the intracellular localization of the channels from the basolateral side to perinuclear components. These results demonstrate that the phosphorylation-dependent scaffolding of the basolateral K^+ channels by MAGI-1a-long participates in the renal regulation of the fluid and electrolyte homeostasis.

Kidney is the essential organ for the fluid and electrolyte homeostasis, and the derangement of its function results in life-threatening diseases, including hypertension, the most common disease in industrialized societies (1–3). The Mendelian form abnormalities have provided clues to pathophysiology of many diseases, and recent genetic analysis revealed that the Na^+ reabsorption in distal renal tubules participates in the pathogenesis of hypertension (4, 5).

The process of the Na^+ reabsorption in distal renal tubules is the result of coordinated electrolyte transports across the renal epithelia (5, 6). In the epithelia, Na^+ efflux occurs actively via basolateral Na^+/K^+-ATPases, whereas apical pathways passively mediate Na^+ influx. Different pathways mediate the apical Na^+ influx in each segment of the tubules as follows: Na^+-K^+-$2Cl^-$ cotransporters in the thick ascending limbs of Henle's loop (TAL),[2] Na^+-Cl^- cotransporters in the distal convoluted tubules (DCT), and Na^+ channels in the connecting tubules and the collecting ducts. Because Na^+/K^+-ATPases induce intracellular K^+ influx with simultaneous Na^+ efflux in these segments, K^+ excretion, *i.e.* K^+ recycling, is essential for the continuance of Na^+ reabsorption (7).

Previously, we showed that the Kir5.1/Kir4.1 heteromer, which is a heteromeric assembly of two inwardly rectifying K^+ channels, composes the principal pathway for the basolateral K^+ recycling in the distal portion of TAL and the DCT (8–10). The functional expression of this heteromer is regulated by the following two motifs in the carboxyl-terminal (CT) portion of the Kir4.1 subunit: (i) dihydrophobic motif for functional cell-surface expression and (ii) PSD-95/Dlg/ZO-1 (PDZ)-binding motif for basolateral localization (11). Therefore, the renal tubules are believed to regulate the basolateral K^+ recycling by the mechanism that recognizes these motifs, and the mechanism is a key factor for the renal regulation of Na^+ and K^+ homeostasis (6, 12).

This study reports that an isoform of membrane-associated guanylate kinase with inverted domain structure 1 (MAGI-1a) functions as a scaffolding protein for the channels that compose the basolateral K^+ recycling pathway.

EXPERIMENTAL PROCEDURES

Yeast Two-hybrid Screening and Cloning—The CT of rat Kir4.1, which is a fragment of 105 amino acid residues, was fused to a GAL4 DNA-binding domain, and 500,000 clones of a rat kidney cDNA library were screened by using the Matchmaker GAL4 two-hybrid system (Takara Bio Clontech) according to the manufacturer's instructions. The sequence of several clones showed high homology to the sequence of the CT domain of mouse MAGI-1a. The full-length of rat MAGI-1a isoforms, MAGI-1a-long and MAGI-1a-short, was cloned by PCR from rat kidney cDNA with

* This work was supported by grants-in-aid for scientific research from the Ministry of Education, Culture, Sports, Science, and Technology of Japan (to M. T., T. A., and S. I.), by grants from Mishima Kaiun Memorial Foundation (to M. T.), Mochida Memorial Foundation for Medical and Pharmaceutical Research (to M. T.), Japan Heart Foundation/Pfizer Japan Inc. grant for cardiovascular disease research (to M. T.), and Salt Science Research Foundation Grants 0639 and 0734 (to M. T.). The costs of publication of this article were defrayed in part by the payment of page charges. This article must therefore be hereby marked "*advertisement*" in accordance with 18 U.S.C. Section 1734 solely to indicate this fact.

The nucleotide sequence(s) reported in this paper has been submitted to the GenBank™/EBI Data Bank with accession number(s) AY598952 and AY598951.

[S] The on-line version of this article (available at http://www.jbc.org) contains supplemental Figs. S1–S3.

[1] To whom correspondence should be addressed: Division of Nephrology, Hypertension, and Endocrinology, Dept. of Medicine, Tohoku University Graduate School of Medicine, 1-1 Seiryo-cho, Aoba-ku, Sendai 980-8574, Japan. Fax: 81-22-717-7168; E-mail: mtanemoto-tky@umin.ac.jp.

[2] The abbreviations used are: TAL, thick ascending limb; DCT, distal convoluted tubule; PDZ, PSD-95/Dlg/ZO-1; MDCK, Madin-Darby canine kidney; HEK, human embryonic kidney; FITC, fluorescein isothiocyanate; GST, glutathione *S*-transferase; PKA, protein kinase A; RT, reverse transcription; Ni-NTA, nickel-nitrilotriacetic acid; WT, wild type; CT, carboxyl terminus; GFP, green fluorescent protein.

the primer pairs of 5'-ATGTCGAAAGTGATCCAGAA-3' and 5'-TCATGGAGTCATGCCAGGGAAGG-3'. For expression analysis of MAGI-1a isoforms in rat tissues, we performed PCR on Rat MTC Panel I (Clontech) using the primer pairs of 5'-ATGTCGAAAGTGATCCAGAA-3' and 5'-CCGAGGGTCTAACCATGATG-3'.

Construct of Fusion Proteins and Deletion/Point Mutants—Mammalian cell expression vectors that contain green fluorescent protein (GFP)-tagged Kir4.1 (GFP-Kir4.1), its deletion/point mutants, and MAGI-1a isoforms were constructed as described previously (11). Polyhistidine-tagged CT81 segments with and without mutation were constructed by subcloning PCR-amplified DNA fragments into the expression vector pcDNA4/HisMaxC (Invitrogen).

Transient Expression in Mammalian Cell Lines—Human embryonic kidney (HEK)293T cells and Madin-Darby canine kidney (MDCK) cells were cultured in Dulbecco's modified Eagle's medium containing 10% fetal bovine serum (both from Invitrogen) and were transfected with the expression vectors by using Lipofectamine 2000 (Invitrogen) according to the manufacturer's protocol. MDCK cells were plated on polycarbonate Millicell transwell filters (Millipore, Bedford, MA) prior to transfection. The further analysis of expressed proteins was usually conducted at 48–72 h after transfection as described previously (13).

Antibodies—A polyclonal anti-MAGI-1 antibody was raised in rabbits against the synthetic peptide SFTADSGDQDEPTLQEATL that corresponds to amino acids 258–267 of MAGI-1a-long (amino acids 39–58 of MAGI-1a-short). A polyclonal anti-K^+-channel Kir4.1 antibody (Sigma), BD Living Colors™ Av peptide antibodies (Takara Bio Clontech), Alexa Fluor 594 anti-rabbit IgG $(Fab')_2$ (Molecular Probes, Eugene, OR), and fluorescein isothiocyanate (FITC)-labeled anti-rabbit IgG (Dako, Glostrup, Denmark) were purchased.

Protein Precipitation and Immunoblotting Analysis—Protein precipitation and immunoblotting analysis were performed as described previously (8). The antibody-pretreated protein A-Sepharose (Amersham Biosciences) was used for immunoprecipitation. The protein A-Sepharose pretreated with preimmune rabbit IgG was used for negative control. Ni-NTA-agarose (Qiagen, Hilden, Germany) was used for polyhistidine-tagged fragments precipitation. The precipitated proteins were analyzed by immunoblotting and detected by SuperSignal West Dura Extended Duration Substrate (Pierce). The intensity of the detected bands was calculated using NIH Image software (National Institutes of Health, Bethesda).

Immunohistochemical Analysis—Adult Sprague-Dawley rats were anesthetized in accordance with the regulations of the Animal Care Committee of our institute, and then perfused transcardially with 0.9% saline followed by perfusion with 4% paraformaldehyde in 0.1 M sodium phosphate (pH 7.4). After dehydration, the kidney was embedded in paraffin, and thin sections of 3–5-μm thickness were obtained. After deparaffinization and rehydration, the sections were immunostained and then observed using a confocal microscope (model LSM 5 PASCAL, Carl Zeiss Co., Ltd., Jena, Germany) as described previously (10). In brief, after incubation in blocking buffer containing 5% normal goat serum, the sections were incubated with the anti-Kir4.1 antibody followed by incubation with an excess (1:20 dilution) of Alexa Fluor 594 anti-rabbit IgG $(Fab')_2$ to saturate the epitopes of the primary antibody. After being washed extensively with phosphate-buffered saline, the sections were subsequently incubated with the anti-MAGI-1 antibody followed by incubation with FITC-labeled anti-rabbit IgG at 1:100 dilution. The sections were observed by a confocal microscope after extensive washing with phosphate-buffered saline. The saturation of the first primary antibody was confirmed by the preliminary experiment that did not detect any labeling with FITC by subsequent incubation with control rabbit IgG.

Salt Loading for Animals—At 8 weeks of age, the diet of rats was switched from a 0.3% NaCl to an 8% NaCl (high salt)-containing diet for 2 weeks. Control rats were fed with a 0.3% NaCl diet throughout the experiments.

Glutathione S-Transferase (GST) Pulldown Analysis—GST fusion proteins of several CT segments of MAGI-1a were constructed by subcloning PCR-amplified DNA fragments into the bacterial expression vector pGEX-5X3 (Amersham Biosciences), and each fusion protein was purified on glutathione-Sepharose™ 4B (Amersham Biosciences) according to the manufacturer's protocol. GFP-Kir4.1 resolved as described above was incubated with these purified GST fusion proteins and then analyzed by immunoblotting as described previously (13).

Protein Kinase A (PKA) Phosphorylation—Experiments involving PKA stimulation were performed using a cAMP mixture containing 5 μM forskolin, 100 μM 8-Br-cAMP, and 100 μM 3-isobutyl-1-methylxanthine. The cAMP mixture was applied for 10 min until just before further preparation. For the inhibition of PKA, a PKA-specific blocker, *N*-(2([3-(4-bromophenyl)-2-propenyl]amino)-ethyl)-5-iso-quinolinesulfonamide (H89) (Seikagaku Corp., Tokyo, Japan) was applied at a concentration of 1.0 μM from 3 min prior the application of the mixture (14).

Electrophysiological Recordings—Channel activity was analyzed with the patch clamp method in whole-cell configuration as described previously (8). In brief, the resistance of patch electrodes, when filled with the pipette solution (140 mM KCl, 1 mM $MgCl_2$, 1 mM $CaCl_2$ and 5 mM HEPES-KOH (pH 7.4)) was adjusted to 1–2 megohms. Currents were elicited on GFP-Kir4.1-transfected HEK293T cells by voltage steps in the bath solution containing 120 mM NaCl, 20 mM KCl, 5 mM EGTA, 2 mM $MgCl_2$, and 5 mM HEPES-KOH (pH 7.3) using a patch clamp amplifier (Axopatch 200B, Axon Instruments, Union City, CA). Data were analyzed by pCLAMP 9 (Axon Instruments), and barium (3 mM)-sensitive components of the currents were recorded as K^+ currents.

Reverse Transcription (RT)-PCR Analysis—Total RNA was extracted from MDCK cells using TRIzol reagent (Invitrogen) and reverse-transcribed with $(dT)_{12-18}$ primer by using Superscript II RT (Invitrogen). MAGI-1a expression was detected by PCR using a primer pair 5'-CCAGTAATTGGGAAATCACACC-3' and 5'-CCGCCTCAGAAACAGACGGAC-3', which spans introns to distinguish these sequences from the genomic DNA. The PCR products were analyzed by agarose gel electrophoresis and visualized by staining with ethidium bromide.

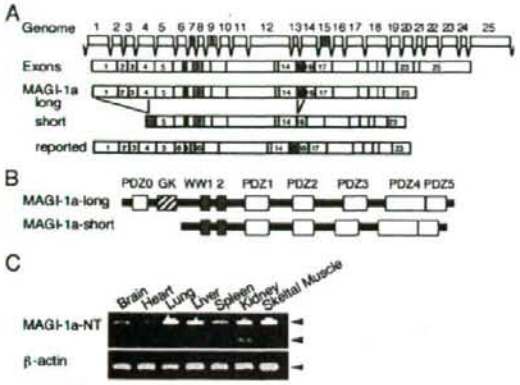

FIGURE 1. **MAGI-1a isoforms expressed in rat kidney.** *A*, exons of MAGI-1 deduced from the sequence in a genomic data base. Arrangements of exons in MAGI-1a isoforms are schematically shown. Splice sites identified in this study are indicated in *gray*. *B*, putative domain structures of MAGI-1a-long and MAGI-1a-short. *C*, expression of MAGI-1a isoforms in rat tissues examined by RT-PCR. *Arrowheads* in the *upper panel* indicate the expected sizes for MAGI-1a-long (*upper band*) and MAGI-1a-short (*lower band*). *Arrowhead* in the *lower panel* indicates the expected sizes for β-actin. *NT*, amino terminus.

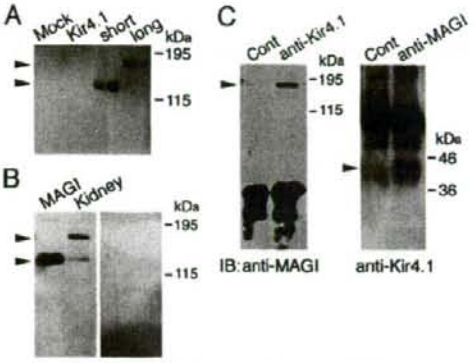

FIGURE 2. **Intrarenal interaction of MAGI-1a-long and Kir4.1.** *A*, immunoreactivity of the anti-MAGI-1 antibody raised in this study. The antibody specifically detected MAGI-1a isoforms expressed in HEK293T cells. *Arrowheads* indicate the sizes for MAGI-1a-short (*lower band*) and MAGI-1a-long (*upper band*). A representative result of immunoblotting is shown ($n = 3$). *Mock*, *Kir4.1*, *short*, and *long* indicate cell lysates from HEK293T cells transfected with mock vector, Kir4.1, MAGI-1a-short, and MAGI-1a-long, respectively. *B*, renal expression of MAGI-1a isoforms examined by immunoblotting with anti-MAGI-1 antibody. Both MAGI-1a-long (*upper arrowhead*) and MAGI-1a-short (*lower arrowhead*) were expressed in rat kidney. The pre-absorption by the antigenic peptide specifically reduced the detection by the antibody (*right panel*). Representative results of immunoblotting are shown ($n = 3$ for each). *MAGI*, lysate from MAGI-1a-short transfected HEK293T cells; *Kidney*, lysate from rat kidney. *C*, mutual immunoprecipitation of MAGI-1a-long and Kir4.1 from rat kidney lysate. Immunoprecipitants of preimmune rabbit IgG (*Cont*), anti-Kir4.1 antibody (*anti-Kir4.1*), and anti-MAGI-1 antibody (*anti-MAGI*) were detected by the antibodies indicated. *Arrowheads* indicate the predicted size of MAGI-1a-long (*left panel*) and Kir4.1 (*right panel*). Representative results of immunoblotting (*IB*) are shown ($n = 3$ for each).

Cytological Observation—Cytological observation was performed as described previously (11). Especially in experiments with MDCK cells, formation of tight junction between cells after confluent growth was confirmed by the expression of a typical protein of tight junction, ZO-1, on the top of a lateral wall. Immunostaining was performed in phosphate-buffered saline containing 0.05% Triton X-100, 5% bovine serum albumin, and 1% normal goat serum.

Statistical Analysis—The intensity of the bands in immunoblotting analysis was expressed as means ± S.D. Comparison was performed by the paired two-tailed Student's *t* test. Probability values of $p < 0.01$ were considered to be statistically significant.

RESULTS

Identification of MAGI-1a as a Scaffolding Protein for Kir4.1 in the Kidney—Two isoforms of MAGI-1a were identified from rat kidney cDNA (supplemental Fig. S1). The longer one, named MAGI-1a-long (GenBank™ accession number AY598952), had two short inserts to the reported MAGI-1a (before and after the second WW domain). The shorter one, named MAGI-1a-short (GenBank™ accession number AY598951), had two splice-out portions from MAGI-1a-long (in the amino terminus and between PDZ2 and PDZ3) (Fig. 1*A* and supplemental Fig. S1). As a consequence of the splice-out, MAGI-1a-short lacked the amino-terminal PDZ domain (so-called PDZ0) and the guanylate kinase domain (Fig. 1*B*). Analysis by PCR on rat tissue cDNA revealed that the kidney expressed both MAGI-1a-long and MAGI-1a-short, and MAGI-1a-short was expressed only in the kidney among the tissues examined (Fig. 1*C* and supplemental Fig. S2).

Expression of MAGI-1a-long-Kir4.1 Complex in Renal Distal Tubules—Using the anti-MAGI antibody, which specifically recognized MAGI-1a-short and MAGI-1a-long expressed in HEK293T cells (Fig. 2*A*), we confirmed the expression of both MAGI-1a isoforms in the kidney (Fig. 2*B*). The antibody detected two bands in the lysate from the membrane fraction of rat kidney (Fig. 2*B*, *left panel*), the identical size of MAGI-1a-short (*lower band*) and the predicted size of MAGI-1a-long (*upper band*). The antibody pre-absorption by the antigenic peptide reduced the detection and almost eliminated these bands (Fig. 2*B*, *right panel*).

Using the antibody, we next examined the intrarenal interaction between MAGI-1a isoforms and Kir4.1. In the immunoprecipitant with the anti-Kir4.1 antibody, a single band was detected from the rat kidney lysate by the anti-MAGI-1 antibody (*left panel* in Fig. 2*C*). The size of the band indicated that the isoform coprecipitated with Kir4.1 was MAGI-1a-long. The immunoprecipitant with the anti-MAGI-1 antibody also contained Kir4.1 (*right panel* in Fig. 2*C*). The mutual coprecipitation of MAGI-1a-long and Kir4.1 indicated their intrarenal interaction.

The intrarenal MAGI-1a-long/Kir4.1 interaction was further supported by immunohistochemical analysis (Fig. 3*A*). The immunoreactivity against the anti-MAGI-1 antibody was detected in the tubules that expressed Kir4.1, and coimmunostaining with the anti-Kir4.1 antibody showed the colocalization of MAGI-1a isoforms with Kir4.1 on the basolateral side in these tubules. The expression of MAGI-1a isoforms on the basolateral side was confirmed by the single staining with the anti-MAGI-1 antibody (supplemental Fig. S3).

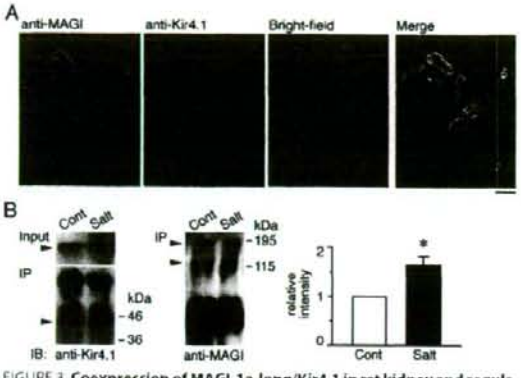

FIGURE 3. **Coexpression of MAGI-1a-long/Kir4.1 in rat kidney and regulation of their interaction by dietary amount of NaCl.** *A*, coimmunostaining of rat kidney with the anti-MAGI-1 antibody (*green*) and the anti-Kir4.1 antibody (*red*). A representative result of immunostaining is shown ($n = 3$). MAGI-1a was colocalized with Kir4.1 on the basolateral side of distal tubules in the cortex. *Scale bar*, 50 μm. *B*, increased intrarenal MAGI-1a-long/Kir4.1 interaction in the salt-loaded rats. *Left* and *middle panels* show representative results of immunoblotting (*IB*) ($n = 4$ for each). More Kir4.1 was coprecipitated with MAGI-1a in the kidney of the salt-loaded rat than the control, although nearly the same amount of Kir4.1 is expressed in both (*left panels*). The antibody used for coprecipitation precipitated a same amount of MAGI-1 isoforms in the control and salt-loaded rats (*middle panel*). *Bar graph* shows the relative intensity of the coprecipitated Kir4.1 in the salt-loaded rats to that in the control ($n = 4$; *, $p < 0.01$). *Cont*, control; *Salt*, salt load; *IP*, immunoprecipitation.

Effects of High Salt Diet on Intrarenal MAGI-1a-long/Kir4.1 Interaction—We next examined the effect of high salt diet (salt load), which could suppress mineralocorticoid secretion, on the intrarenal MAGI-1a-long/Kir4.1 interaction (Fig. 3*B*). The salt load increased the interaction, although it did not increase the amount of Kir4.1 expressed in the kidney. More Kir4.1 was coprecipitated with the same amount of MAGI-1a-long in the kidney of the salt-loaded animals than the control (relative amount: 1.65 ± 0.17, $p = 0.005$).

Interacting Domains of MAGI-1a-long and Kir4.1—Using GST pulldown, we analyzed the regions for the MAGI-1a-long/Kir4.1 interaction. The CT domain of MAGI-1a-long that was identified by the yeast two-hybrid screening could interact with Kir4.1 (Fig. 4*A*). Sequential deletion of the domain from the CT end showed that the deletion of the fifth PDZ domain (PDZ5) disrupted the interaction, which indicates that the PDZ5 domain is essential for MAGI-1a-long to interact with Kir4.1.

The deletion of the PDZ-binding motif in Kir4.1 disrupted the MAGI-1a-long/Kir4.1 interaction (Fig. 4*B*). A single mutation of serine 377, the critical residue in the motif, to alanine (S377A) or aspartic acid (S377D) also disrupted the interaction. These results indicated that the PDZ-binding motif of Kir4.1 was essential for the MAGI-1a-long/Kir4.1 interaction and confirmed that the interaction was PDZ-dependent.

Regulation of the MAGI-1a-long/Kir4.1 Interaction—The PDZ dependence of the MAGI-1a-long/Kir4.1 interaction was further confirmed in HEK293T cells. In HEK293T cells, as well as in the GST pulldown, the Kir4.1 with wild-type (WT) CT portion could interact with MAGI-1a-long, but the deletion of the PDZ-binding motif in Kir4.1 disrupted the mutual interaction between MAGI-1a-long and Kir4.1 (Fig. 5*A*).

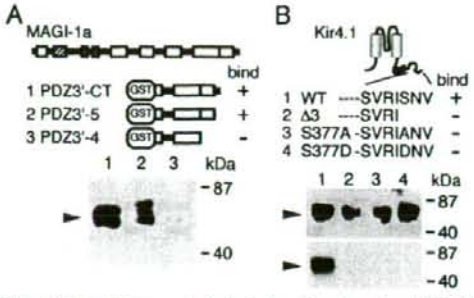

FIGURE 4. **GST pulldown analysis for interacting domains of MAGI-1a-long and Kir4.1.** *A*, GST pulldown of GFP-Kir4.1 by CT segments of MAGI-1a. *Schema* shows each GST fusion construct and summarizes its binding to Kir4.1. *Lower panel* shows a representative result of GST pulldown ($n = 3$). Fusion proteins that contain PDZ5 interacted with Kir4.1; however, deletion of PDZ5 diminished the interaction. *B*, GST pulldown analysis of GFP-Kir4.1 mutants by PDZ3'-CT segment of MAGI-1a. *Schema* shows the sequence of CT of each GFP-Kir4.1 mutant and summarizes its binding to MAGI-1a-long. *Panels* show representative results of expression (*upper panel*) and pulldown analysis (*lower panel*) ($n = 3$). Deletion (Δ3) and single mutations (S377A, S377D) in the PDZ-binding motif disrupted the interaction.

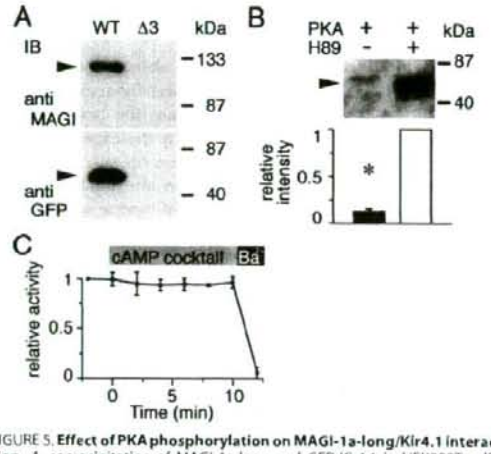

FIGURE 5. **Effect of PKA phosphorylation on MAGI-1a-long/Kir4.1 interaction.** *A*, coprecipitation of MAGI-1a-long and GFP-Kir4.1 in HEK293T cells. *Panels* show representative results of immunoprecipitation (by anti-GFP antibody (*upper panel*) and anti-MAGI-1 antibody (*lower panel*)). Mutual interaction of Kir4.1 (wild-type, *WT*) and MAGI-1a-long was disrupted by deletion of the PDZ-binding motif (Δ3) from Kir4.1. *IB*, immunoblot. *B*, disruption of the MAGI-1a-long/Kir4.1 interaction by PKA phosphorylation. *Panel* shows a representative result of immunoprecipitation of Kir4.1 by anti-MAGI-1 antibody. *Bar graph* shows the relative intensity of the Kir4.1 coprecipitated with MAGI-1a-long under PKA stimulation compared with under co-inhibition by H89 ($n = 3$; *, $p < 0.01$). The conditions of incubation are indicated in the panel above. The disruption was impeded by H89, a PKA-specific inhibitor. *PKA*, incubation with cAMP mixture; *H89*, co-inhibition by H89. *C*, effect of PKA phosphorylation on Kir4.1 channel activity. The *graph* summarizes the relative K^+ current of Kir4.1 under conditions indicated above the graph ($n = 3$). No reduction of the channel activity was observed during PKA phosphorylation. *CAMP cocktail*, cAMP mixture in bath solution; Ba^{2+}, 3 mM barium in bath solution.

In the GST pulldown analysis, the induction of a phosphorylated state-mimicking mutation in serine 377 (S377D) disrupted the MAGI-1a-long/Kir4.1 interaction, which indicated that serine 377 phosphorylation affected the interaction. Because serine 377 of Kir4.1 is a putative site for phosphoryla-

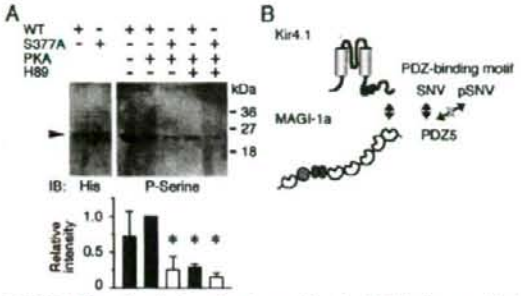

FIGURE 6. **Phosphorylation of serine residue in PDZ-binding motif of Kir4.1.** *A*, PKA phosphorylation of CT portion of Kir4.1. Ni-NTA-agarose-precipitated polyhistidine-tagged CT81 segment of Kir4.1 expressed in HEK293T cells was detected by antibodies indicated. *His*, anti-polyhistidine antibody; *P-Serine*, anti-phosphoserine antibody. Sequence of segments and condition of treatments are indicated above panels. *S377A*, mutant with serine 377 to alanine; *PKA*, stimulation with cAMP mixture; *H89*, inhibition by H89. Representative immunoblots (*IB*) are shown in *upper panels*, and relative intensity is summarized in the *bar graph* (mean ± S.D., $n = 4$; *, $p < 0.01$ compared with WT/PKA + /H89−). *B*, schematic summary of MAGI-1a-long/Kir4.1 interaction. Only PDZ-binding motif of Kir4.1 with unphosphorylated serine 377 can bind to PDZ5 of MAGI-1a-long.

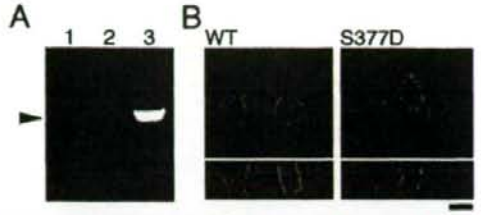

FIGURE 7. **PDZ dependence of K^+ channel localization in MDCK cells.** *A*, expression of MAGI-1 isoforms in MDCK cells. RT-PCR analysis for the expression of MAGI-1 in MDCK cells by using a MAGI-1-specific primer pair. A representative result of the analysis is shown ($n = 3$). *Lane 1*, cDNA of MDCK cells; *lane 2*, RT(−) total RNA of MDCK cells; *lane 3*, cDNA of MAGI-1a-long as a positive control. *B*, intracellular localization of GFP-Kir4.1 mutants in MDCK cells. A representative result of the localization is shown ($n = 5$). Whereas wild-type (*WT*) GFP-Kir4.1 is predominantly localized on basolateral side, single phosphorylation-mimic mutation (serine 377 to aspartic acid; S377D) induced perinuclear localization. *Scale bar*, 10 μm.

tion by PKA, we further examined the effects of PKA phosphorylation on the MAGI-1a-long/Kir4.1 interaction in HEK293T cells (Fig. 5*B*). The interaction was disrupted during 10 min of incubation with the cAMP mixture, whereas a PKA-specific inhibitor, H89, overcame this disruption. Compared with the amount of Kir4.1 coprecipitated with MAGI-1a-long after simultaneous inhibition with H89, the amount after PKA stimulation was significantly low (0.13 ± 0.03, $p < 0.001$).

Interestingly, the current amplitude of Kir4.1 assessed by patch clamp did not change during the 10-min cAMP mixture application, which sufficiently disrupted the PDZ-dependent interaction with MAGI-1a-long; the amplitude after the 10-min application relative to that before the application was 0.96 ± 0.05 (Fig. 5*C*).

Phosphorylation of Serine 377 in the PDZ-binding Motif—We further examined PKA phosphorylation on the CT81 amino acid residues of Kir4.1 (CT81 segment) (Fig. 6*A*). Whereas Ni-NTA-agarose precipitated the same amount of the WT and S377A polyhistidine-tagged CT81 segments, the WT segment instead of the S377A segment was more efficiently serine-phosphorylated by the cAMP mixture application in the H89-inhibitory manner. Compared with the intensity of phosphoserine on the WT segment, the intensity on the S377A segment was statistically significantly weak (0.25 ± 0.19, $p = 0.004$), and the reduction in the intensity by simultaneous H89 inhibition was significant only in the WT segment (WT, 0.29 ± 0.05, $p < 0.001$; S377A, 0.15 ± 0.05, $p = 0.305$). These results indicated that the serine 377 in the PDZ-binding motif was the residue that was PKA-phosphorylated. The motif with unphosphorylated but not phosphorylated serine 377 could interact with the PDZ5 of MAGI-1a (schematically summarized in Fig. 6*B*).

In the absence of extra activation for PKA, the intensity of phosphoserine on the WT segment changed widely in each experiment (ranging from 0.33 to 1.13). However, the intensity without the extra activation was generally weaker than the intensity with the extra activation (0.72 ± 0.34, $p = 0.201$).

Effect of Kir4.1 Phosphorylation on Intracellular Localization—We further examined the effect of phosphorylation on the intracellular localization of Kir4.1 in renal tubular cells by using a cell line derived from the renal tubule, MDCK cells. RT-PCR analysis by using a specific primer pair for MAGI-1 revealed the expression of MAGI-1 isoform(s) in MDCK cells (Fig. 7*A*). In MDCK cells, Kir4.1 showed the predominant localization on the basolateral side, but the induction of a phosphorylation-mimicking single mutation at serine 377 (S377D) induced the perinuclear localization (Fig. 7*B*). These results indicated that the PDZ-dependent interaction with MAGI-1 isoform(s), which is disrupted by the phosphorylation of serine 377 in the PDZ-binding motif, participated in the basolateral localization of Kir4.1 in renal tubular cells.

DISCUSSION

In this study, we revealed that a scaffolding protein, MAGI-1a-long, interacts with Kir4.1 on the basolateral side of distal renal tubules. The interaction is affected by dietary amount of NaCl and regulated by phosphorylation of the PDZ-binding motif of Kir4.1.

Previously, we showed that Kir4.1 is a subunit of the basolateral K^+ channels (a pathway of basolateral K^+ recycling for Na^+ reabsorption) in distal renal tubules (8, 9), and that the PDZ-binding motif of this subunit participates in the proper expression of the channels (10, 11). Therefore, our findings in this study indicate that MAGI-1a-long participates in the basolateral localization of the K^+ channels in these tubules; this is similar to the PDZ-dependent localization of other membrane proteins by scaffolding proteins (15).

We detected the expression of MAGI-1 isoforms in the renal tubules but not in the glomerulus. The intrarenal interaction of MAGI-1a-long with Kir4.1, which is not expressed in the glomerulus but in distal renal tubules (10, 16), confirmed the tubular expression of MAGI-1 isoforms. In a previous report, another MAGI-1-specific antibody also detected tubular but not intraglomerular expression of MAGI-1 (17). However, there are several reports that show intraglomerular expression of MAGI-1 (18–20). In these previous reports, the antibodies that were raised against other members of scaffolding proteins (19, 20) or that recognized several proteins with sizes different

from MAGI-1 (18) were used, because they could detect MAGI-1. Therefore, intraglomerular immunoreactivity with these antibodies could be against some other proteins, such as a synaptic scaffolding molecule, but not MAGI-1 (21). It is also possible that isoform(s) of MAGI-1 without the amino-terminal portion are expressed in the glomerulus, because we raised the anti-MAGI-1 antibody against an amino acid sequence on the amino-terminal portion of MAGI-1a in this study.

In the renal tubules, the MAGI-1 expression was detected on the luminal side in addition to the basolateral side where MAGI-1a-long was colocalized with Kir4.1. Because MAGI-1a-short is the renal MAGI-1 isoform that did not interact with Kir4.1, it would be the isoform expressed on the luminal side. Although we could not clarify the precise localization of the isoforms, they probably have different intracellular localizations, *i.e.* MAGI-1a-short on the luminal side and MAGI-1a-long on the basolateral side. The PDZ0 and guanylate kinase domain, the domains that only MAGI-1a-long contains, might be responsible for the different localization (15). The different localization would make it possible for MAGI-1a-long but not MAGI-1a-short to interact with Kir4.1 *in vivo* in the kidney.

The mechanism for *in vivo* interaction of Kir4.1 with the basolaterally expressed MAGI-1a-long but not the luminally expressed MAGI-1 isoforms has not been clarified. However, we propose two possible mechanisms. (i) PDZ5 of the luminally expressed MAGI-1 isoforms is preoccupied *in vivo* by other proteins (18, 22). (ii) The basolateral K^+ channels are specifically delivered to the basolateral side by the mechanism that is not clarified yet (12, 23).

The MAGI-1a-long/Kir4.1 interaction was disrupted by phosphorylation. Phosphorylation is thought to take place on the serine 377 in the PDZ-binding motif, and only the PDZ-binding motif with the unphosphorylated serine 377 could interact with the PDZ5 of MAGI-1a-long (Fig. 6*B*). Either the phosphorylation or the amino acid mutation (to alanine or aspartic acid, which mimics the phosphorylated serine (24, 25)) of the serine 377 disrupted the interaction. In line with our findings, phosphorylation of PDZ-binding motifs in other proteins also changes their interaction with scaffolding proteins and affects their intracellular localization (26, 27).

Interestingly, although the PKA phosphorylation disrupted the MAGI-1a-long/Kir4.1 interaction, it did not change the channel activity of Kir4.1 for a short duration. We previously showed that the PDZ-dependent interaction with scaffolding protein(s) facilitates the localization of the K^+ channels on the intracellular compartments just beneath the cell surface but not on the extracellular surface (10, 11). Because of this intracellular localization, the PKA phosphorylation would not change the channel activity for a short duration. The phosphorylation would regulate the process of intracellular localization that affects the channels ready to be expressed on the cell surface. The channels on the compartments just beneath the cell surface could be functional on demand (7).

Serine residues in the CT portion of Kir4.1 other than serine 377, such as serine 343, could be PKA-phosphorylated (28), and might affect the interaction. Less phosphorylation on a S377A-mutated segment under PKA inhibition than PKA stimulation might reflect PKA phosphorylation of these residues (14). However, the difference is too small ($p = 0.305$) to be considered as the different phosphorylation state of any residues, and serine 377 in the PDZ-binding motif is thought to be the residue that is responsible for the phosphorylation-dependent regulation of the interaction.

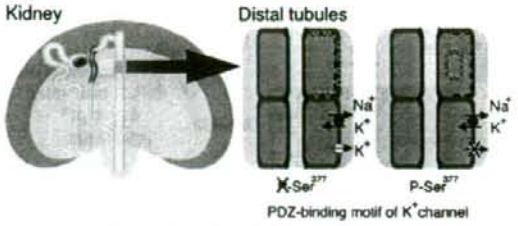

FIGURE 8. **Regulation of basolateral K^+ channels in distal renal tubules.** Phosphorylation-dependent basolateral localization of distal renal tubular K^+ channels is schematically summarized. In the distal portion of TAL and the DCT (indicated by *green* in *left panel*), MAGI-1a-long (indicated by *red dots* in *right panel*) functions as a scaffolding protein for the basolateral K^+ channels. In these tubules, K^+ channels with unphosphorylated PDZ-binding motifs are anchored on basolateral side. Phosphorylation of serine 377 in PDZ-binding motif impedes the channel anchoring and can diminish K^+ reabsorption.

In this study, the activity of PKA, which would have changed widely *in vitro* according to the condition of the cells without extra activation for it, disrupted the MAGI-1a-long/Kir4.1 interaction in HEK293T cells. Therefore, the intracellular signal cascades that affect the activity of PKA *in vivo* could regulate the activity of the basolateral K^+ recycling in distal renal tubules. However, in distal renal tubules, several kinases that can phosphorylate serine residues, such as SGK1, are known to be expressed (29, 30). These kinases might phosphorylate Kir4.1 more efficiently under the conditions that are suitable for their activity. The phosphorylation by these kinases would affect the activity of the basolateral K^+ recycling and regulate the renal Na^+ reabsorption *in vivo* in the kidney (29, 30). Supporting this notion, in this study, the animal fed with the diet that could reduce the activity of SGK1 (31) had the increased intrarenal MAGI-1a-long/Kir4.1 interaction.

Although the results of this study suggest the MAGI-1 isoform(s) participate in the localization of the basolateral K^+ channel in distal renal tubules and MDCK cells, other scaffolding proteins that contain PDZ domain(s) might participate in the localization. On the basolateral side of MDCK cells and mouse distal renal tubules, the dystrophin-associated protein complex that contains several scaffolding proteins with PDZ domain(s), including α-syntrophin, is reported to exist (32, 33). Because α-syntrophin has the PDZ domain that can interact with the PDZ-binding motif of Kir4.1 (34), these proteins might also contribute to the localization of the basolateral K^+ channels in distal renal tubules. The contribution of these scaffolding proteins for the localization of the K^+ channels remains to be clarified by their direct interaction in distal renal tubules.

In conclusion, MAGI-1a-long functions as a scaffolding protein for the distal renal tubular basolateral K^+ channels (Fig. 8). Phosphorylation of the channels impedes the channel scaffolding by MAGI-1a-long and could decrease the basolateral K^+ recycling. These findings suggest that the regulatory pathway for the activity of kinases in renal tubules participates in the distal renal tubular Na^+/K^+ regulation.

REFERENCES

1. Wang, Y., and Wang, Q. J. (2004) *Arch. Intern. Med.* **164,** 2126–2134
2. Psaltopoulou, T., Orfanos, P., Naska, A., Lenas, D., Trichopoulos, D., and Trichopoulou, A. (2004) *Int. J. Epidemiol.* **33,** 1345–1352
3. Gu, D., Reynolds, K., Wu, X., Chen, J., Duan, X., Muntner, P., Huang, G., Reynolds, R. F., Su, S., Whelton, P. K., and He, J. (2002) *Hypertension* **40,** 920–927
4. Wilson, F. H., Disse-Nicodeme, S., Choate, K. A., Ishikawa, K., Nelson-Williams, C., Desitter, I., Gunel, M., Milford, D. V., Lipkin, G. W., Achard, J. M., Feely, M. P., Dussol, B., Berland, Y., Unwin, R. J., Mayan, H., Simon, D. B., Farfel, Z., Jeunemaitre, X., and Lifton, R. P. (2001) *Science* **293,** 1107–1112
5. Lifton, R. P., Gharavi, A. G., and Geller, D. S. (2001) *Cell* **104,** 545–556
6. Meneton, P., Loffing, J., and Warnock, D. G. (2004) *Am. J. Physiol.* **287,** F593–F601
7. Giebisch, G. (2001) *Kidney Int.* **60,** 436–445
8. Tanemoto, M., Kittaka, N., Inanobe, A., and Kurachi, Y. (2000) *J. Physiol. (Lond.)* **525,** 587–592
9. Lourdel, S., Paulais, M., Cluzeaud, F., Bens, M., Tanemoto, M., Kurachi, Y., Vandewalle, A., and Teulon, J. (2002) *J. Physiol. (Lond.)* **538,** 391–404
10. Tanemoto, M., Abe, T., Onogawa, T., and Ito, S. (2004) *Am. J. Physiol.* **287,** F1148–F1153
11. Tanemoto, M., Abe, T., and Ito, S. (2005) *J. Am. Soc. Nephrol.* **16,** 2608–2614
12. Brown, D., and Breton, S. (2000) *Kidney Int.* **57,** 816–824
13. Tanemoto, M., Fujita, A., Higashi, K., and Kurachi, Y. (2002) *Neuron* **34,** 387–397
14. Chijiwa, T., Mishima, A., Hagiwara, M., Sano, M., Hayashi, K., Inoue, T., Naito, K., Toshioka, T., and Hidaka, H. (1990) *J. Biol. Chem.* **265,** 5267–5272
15. Fanning, A. S., and Anderson, J. M. (1999) *Curr. Opin. Cell Biol.* **11,** 432–439
16. Ito, M., Inanobe, A., Horio, Y., Hibino, H., Isomoto, S., Ito, H., Mori, K., Tonosaki, A., Tomoike, H., and Kurachi, Y. (1996) *FEBS Lett.* **388,** 11–15
17. Laura, R. P., Ross, S., Koeppen, H., and Lasky, L. A. (2002) *Exp. Cell Res.* **275,** 155–170
18. Patrie, K. M., Drescher, A. J., Goyal, M., Wiggins, R. C., and Margolis, B. (2001) *J. Am. Soc. Nephrol.* **12,** 667–677
19. Nishimura, W., Iizuka, T., Hirabayashi, S., Tanaka, N., and Hata, Y. (2000) *J. Cell Physiol.* **185,** 358–365
20. Hirabayashi, S., Mori, H., Kansaku, A., Kurihara, H., Sakai, T., Shimizu, F., Kawachi, H., and Hata, Y. (2005) *Lab. Investig.* **85,** 1528–1543
21. Kawajiri, A., Itoh, N., Fukata, M., Nakagawa, M., Yamaga, M., Iwamatsu, A., and Kaibuchi, K. (2000) *Biochem. Biophys. Res. Commun.* **273,** 712–717
22. Dobrosotskaya, I. Y., and James, G. L. (2000) *Biochem. Biophys. Res. Commun.* **270,** 903–909
23. Rothman, J. E. (1994) *Nature* **372,** 55–63
24. Beguin, P., Nagashima, K., Nishimura, M., Gonoi, T., and Seino, S. (1999) *EMBO J.* **18,** 4722–4732
25. Lin, Y. F., Jan, Y. N., and Jan, L. Y. (2000) *EMBO J.* **19,** 942–955
26. Daniels, D. L., Cohen, A. R., Anderson, J. M., and Brunger, A. T. (1998) *Nat. Struct. Biol.* **5,** 317–325
27. Songyang, Z., Fanning, A. S., Fu, C., Xu, J., Marfatia, S. M., Chishti, A. H., Crompton, A., Chan, A. C., Anderson, J. M., and Cantley, L. C. (1997) *Science* **275,** 73–77
28. Pearson, R. B., and Kemp, B. E. (1991) *Methods Enzymol.* **200,** 62–81
29. Alvarez de la Rosa, D., Coric, T., Todorovic, N., Shao, D., Wang, T., and Canessa, C. M. (2003) *J. Physiol. (Lond.)* **551,** 455–466
30. Vitari, A. C., Deak, M., Morrice, N. A., and Alessi, D. R. (2005) *Biochem. J.* **391,** 17–24
31. Hou, J., Speirs, H. J., Seckl, J. R., and Brown, R. W. (2002) *J. Am. Soc. Nephrol.* **13,** 1190–1198
32. Loh, N. Y., Newey, S. E., Davies, K. E., and Blake, D. J. (2000) *J. Cell Sci.* **113,** 2715–2724
33. Kachinsky, A. M., Froehner, S. C., and Milgram, S. L. (1999) *J. Cell Biol.* **145,** 391–402
34. Connors, N. C., Adams, M. E., Froehner, S. C., and Kofuji, P. (2004) *J. Biol. Chem.* **279,** 28387–28392